Annals of Botany **126**: 511–537, 2020
doi: 10.1093/aob/mcz171, available online at www.academic.oup.com/aob

ANNALS OF BOTANY
Founded 1887

REVIEW: PART OF A SPECIAL ISSUE ON FUNCTIONAL-STRUCTURAL PLANT GROWTH MODELLING

Photosynthesis: basics, history and modelling

Alexandrina Stirbet[1], Dušan Lazár[2,*], Ya Guo[3,4] and Govindjee Govindjee[5,*,†]

[1]Anne Burras Lane, Newport News, VA 23606, USA, [2]Department of Biophysics, Center of the Region Haná for Biotechnological and Agricultural Research, Faculty of Science, Palacký University, Šlechtitelů 27, 783 71 Olomouc, Czech Republic, [3]Key Laboratory of Advanced Process Control for Light Industry (Ministry of Education), Jiangnan University, Wuxi 214122, China, [4]University of Missouri, Columbia, MO 65211, USA and [5]Department of Biochemistry, Department of Plant Biology, and Center of Biophysics & Quantitative Biology, University of Illinois at Urbana-Champaign, Urbana, IL 61801, USA
** For correspondence. E-mail gov@illinois.edu or dusan.lazar@upol.cz*
†Since 2019 the legal name of Govindjee is 'Govindjee Govindjee'.

Received: 8 July 2019 Returned for revision: 6 September 2019 Editorial decision: 15 October 2019 Accepted: 21 October 2019
Electronically published: 13 December 2019

• **Background** With limited agricultural land and increasing human population, it is essential to enhance overall photosynthesis and thus productivity. Oxygenic photosynthesis begins with light absorption, followed by excitation energy transfer to the reaction centres, primary photochemistry, electron and proton transport, NADPH and ATP synthesis, and then CO_2 fixation (Calvin–Benson cycle, as well as Hatch–Slack cycle). Here we cover some of the discoveries related to this process, such as the existence of two light reactions and two photosystems connected by an electron transport 'chain' (the Z-scheme), chemiosmotic hypothesis for ATP synthesis, water oxidation clock for oxygen evolution, steps for carbon fixation, and finally the diverse mechanisms of regulatory processes, such as 'state transitions' and 'non-photochemical quenching' of the excited state of chlorophyll *a*.
• **Scope** In this review, we emphasize that mathematical modelling is a highly valuable tool in understanding and making predictions regarding photosynthesis. Different mathematical models have been used to examine current theories on diverse photosynthetic processes; these have been validated through simulation(s) of available experimental data, such as chlorophyll *a* fluorescence induction, measured with fluorometers using continuous (or modulated) exciting light, and absorbance changes at 820 nm (ΔA_{820}) related to redox changes in P700, the reaction centre of photosystem I.
• **Conclusions** We highlight here the important role of modelling in deciphering and untangling complex photosynthesis processes taking place simultaneously, as well as in predicting possible ways to obtain higher biomass and productivity in plants, algae and cyanobacteria.

Key words: Calvin–Benson cycle, chlorophyll *a* fluorescence induction, non-photochemical quenching (of the excited state of chlorophyll *a*), modelling, discoveries in photosynthesis, photosynthetic electron transport, state transitions.

'Complexity is the prodigy of the world. Simplicity is the sensation of the universe. Behind complexity, there is always simplicity to be revealed. Inside simplicity, there is always complexity to be discovered.'

Gang Yu

INTRODUCTION

With limited agricultural land and increasing human population, it is essential to enhance photosynthetic activities. Oxygenic photosynthesis is a very important process, not only because it is the source of our food, fibre and many useful substances, but also because almost all life on the Earth depends on it, either directly or indirectly. Plants, algae and cyanobacteria are oxygenic photosynthetizers that use light energy to generate organic molecules [e.g. glucose ($C_6H_{12}O_6$), sugars, starch] from carbon dioxide (CO_2) and water (H_2O), and release molecular oxygen (O_2) into the atmosphere (for a background on photosynthesis see, Eaton-Rye *et al.*, 2012; Blankenship, 2014; Shevela *et al.*, 2019):

$$6CO_2 + 12H_2\mathbf{O} + \text{light energy} \rightarrow C_6H_{12}O_6 + 6\mathbf{O}_2 + 6H_2O.$$

Note that the above global equation of photosynthesis emphasizes that the oxygen molecules released into the atmosphere originate from water oxidation, not from carbon dioxide, as established using ^{18}O-labelled water (Ruben *et al.*, 1941).

This process starts in the thylakoid membrane (TM) with two light reactions taking place simultaneously at photosystem (PS) II and PSI reaction centres (RCs; for PSII and PSI, see the review by Nelson and Junge, 2015). The light energy absorbed by pigment–protein antenna complexes of the PSs is converted, with very high efficiency, into redox chemical energy; a small part is, however, dissipated as heat (internal conversion), and as chlorophyll (Chl) fluorescence (2–10 %, Latimer *et al.*, 1956). Furthermore, water is oxidized to oxygen, and $NADP^+$ is reduced

to NADPH, and, in addition, ATP is produced (Rabinowitch and Govindjee, 1969; Blankenship, 2014; Shevela *et al.*, 2019). Both NADPH and ATP are then used for CO_2 assimilation in the stroma (for a historical background of the Calvin–Benson cycle, see, Bassham, 2005; Benson, 2005); here, Rubisco (ribulose 1,5-bisphosphate carboxylase/oxygenase) is a key enzyme, which catalyses the fixation of CO_2 on a five-carbon compound, RuBP (ribulose 1,5-*bis*phosphate). A diagram of the photosynthetic apparatus and the electron transport (ET) reactions is shown in Fig. 1.

The availability of high-performance computers and detailed knowledge of the various steps of photosynthesis have provided new opportunities to use mathematical modelling to better understand the dynamics of this process (see reviews by Lazár and Schansker, 2009; Jablonsky *et al.*, 2011; Stirbet *et al.*, 2014). In addition, several studies (Zhu *et al.*, 2010; Long *et al.*, 2006, 2015; Ort *et al.*, 2015; South *et al.*, 2018; Simkin *et al.*, 2019) strongly support the idea that the photosynthetic processes can be improved through genetic engineering to increase the yield potential of various crops (see also Rosenthal *et al.*, 2011; Simkin *et al.*, 2015, 2017; Kromdijk *et al.*, 2016; McGrath and Long, 2016). Furthermore, mathematical modelling can be used to predict opportunities for specific genetic modifications and devise optimized engineering designs to improve photosynthesis (Zhu *et al.*, 2007).

In this review, we first provide a background of oxygenic photosynthesis that forms the basis of its modelling. We then discuss a few selected studies on mathematical models describing photosynthetic processes. Partial reactions of photosynthesis have been often modelled separately, such as: (1) the primary photochemical reactions (e.g. Schatz *et al.*, 1988; Roelofs *et al.*, 1992); (2) water 'splitting' reactions (e.g. Kok *et al.*, 1970; Mar and Govindjee, 1972; Jablonsky and Lazár, 2008; Shen, 2015); (3) reduction of Q_B, the secondary plastoquinone (PQ) acceptor of PSII (e.g. Velthuys and Amesz, 1974; Petrouleas and Crofts, 2005); and (4) the redox reactions of the PQ pool at the Cyt b_6/f complex (which may include the Q-cycle; see e.g. Mitchell, 1975; Cramer *et al.*, 2011). However, in this review we mainly discuss larger models, which include several steps, providing information on complex photosynthetic processes.

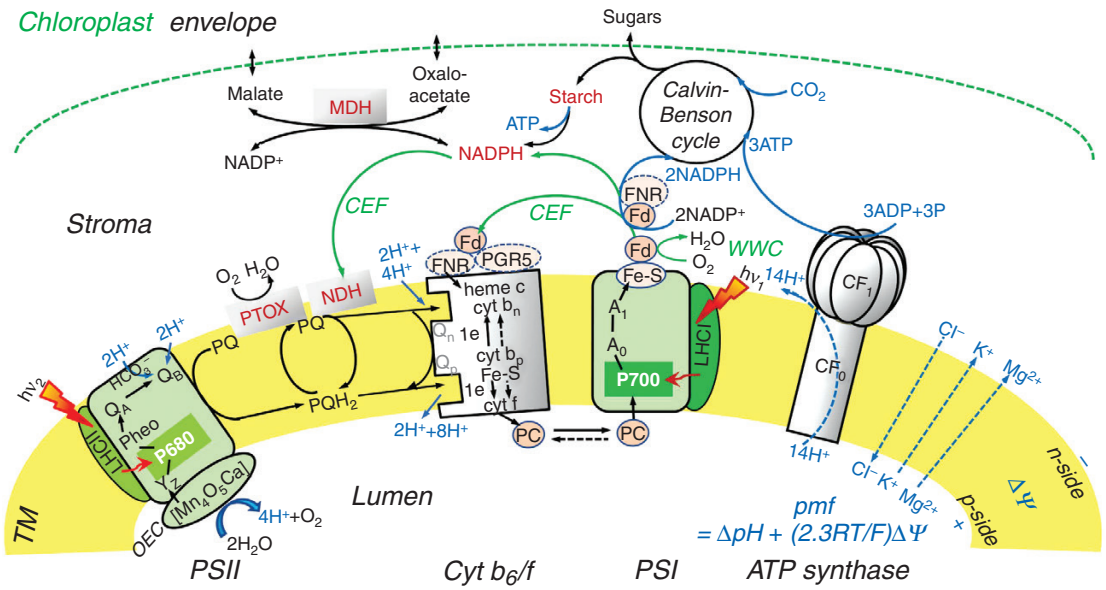

FIG. 1. Diagram of the photosynthetic apparatus and electron transport (ET) pathways in plants and algae. Four major protein complexes in the thylakoid membrane (TM) participate in the production of ATP and nicotinamide adenine dinucleotide phosphate in reduced form (NADPH), needed for the Calvin–Benson cycle to fix CO_2 to produce sugars: two photosystems (PSII and PSI) connected in series via the cytochrome (Cyt) b_6/f, and the ATP synthase. Light is absorbed simultaneously by pigments in the light harvesting complexes of PSI and PSII (LHCI and LHCII); excitation energy is transferred to reaction centre (RC) P700 (in PSI) and P680 (in PSII), where primary charge separation takes place, initiating a chain of redox reactions. PSII functions as a water/PQ (photo)-oxidoreductase, which has a manganese complex [Mn_4O_5Ca], and a tyrosine-161 (Y_Z), located on D1 protein on the electron donor side, as well as pheophytin (Pheo), plastoquinones Q_A and Q_B, and a non-haem (heme) iron binding a bicarbonate ion (HCO_3^-) on the electron acceptor side. By contrast, PSI is a plastocyanin (PC)/ferredoxin (Fd) (photo)-oxidoreductase; it uses reduced PC as an electron donor, and a particular Chl *a* molecule (A_0), vitamin K_1 (A_1), and three non-haem iron–sulfur centres (shown in the figure as Fe-S) are on the acceptor side of PSI. The Cyt b_6/f complex includes a Cyt f, a Rieske iron–sulfur protein (Fe-S), two cytochromes b (Cyt b_p and Cyt b_n) that participate in the oxidation and reduction of PQH_2 and PQ: PQH_2 is oxidized at the Q_p-site by Cyt b_p, while PQ is reduced at the Q_n-site by Cyt b_n. The Q_p- and Q_n-sides are also called Q_o- and Q_i-sides, respectively. Besides the linear ET flow from water to $NADP^+$, there are several pathways leading to electron donation to alternative electron acceptors: cyclic electron flow (CEF) around PSI mediated by Fd (involving Fd-$NADP^+$-reductase, FNR, and a proton gradient regulator, PGR5), or NADPH (via NADPH dehydrogenase, NDH); water–water cycle (WWC); chlororespiration (through the plastid terminal oxidase, PTOX); and the malate valve (through malate dehydrogenase, MDH). The proton motive force (*pmf*) [consisting of the proton concentration difference (ΔpH) and the electric potential ($\Delta\Psi$) across TM] is used by ATP synthase to produce ATP from ADP and phosphate (P_i); in the *pmf* formula, *R* is the gas constant, *F* is the Faraday constant, and *T* is the absolute temperature (in K). Modified from Alric (2010).

PHOTOSYNTHESIS IN PLANTS, ALGAE AND CYANOBACTERIA: SOME BASICS

Early discoveries

Not much was known about photosynthesis before the 20th century; for earlier discoveries in photosynthesis see chapter 2 in Rabinowitch (1945) and the timeline in Govindjee and Krogmann (2004). The key discoveries were as follows (see chapter 1 in Rabinowitch and Govindjee, 1969): Jan van Helmont (1648) showed that plant growth was mainly from the water that plants had absorbed; it was only later that Nicolas Théodore de Saussure (1804) clearly showed that water was an essential reactant of photosynthesis. Joseph Priestley (1776) showed, in elegant experiments, that plants produced 'oxygen' (then called de-phlogisticated air) needed by a mouse to live, whereas Jan Ingen-Housz (1773) convincingly established that light was necessary for photosynthesis. The role of CO_2 in photosynthesis was shown by Jean Senebier (1782), whereas the synthesis of starch was shown by Julius von Sachs (1862, 1864). However, the involvement of chlorophyll (Chl) in this process has a long history. For some of the earliest concepts, we must remember to mention Pierre Joseph Pelletier and Joseph Bienaimé Caventou (1817, 1818), and René Joachim Henri Dutrochet (1837). However, Theodor Engelmann (1882) provided the first action spectrum of photosynthesis, showing that red and blue light, absorbed by Chl, produce oxygen (see figure 1.1 and its description in Shevela *et al.*, 2019).

Physiological and biochemical advances

An understanding of how photosynthesis functions began only after 1900, but by 1960 a basic model at the molecular level, including generation of NADPH and ATP as well as the steps leading to the assimilation of CO_2 to produce carbohydrates, was established (see Govindjee and Krogmann, 2004; Govindjee *et al*., 2005; Nickelsen, 2016).

By measuring photosynthesis as a function of light intensity, Frederick Frost Blackman (1905) suggested that photosynthesis consists of two separate phases: a light-dependent phase (i.e. so-called 'light' reactions), and a temperature-dependent biochemical phase (so-called 'dark' reactions, or 'Blackman reaction'; see Warburg and Uyesugi, 1924). However, because CO_2 fixation uses NADPH and ATP, formed in the light phase, these so-called 'dark' reactions are also light-dependent. Moreover, many enzymes, involved in CO_2 assimilation reactions, function only when they are 'light-activated', being controlled through the ferredoxin:thioredoxin reductase (FTR) system (see reviews by Buchanan *et al.*, 2002; Nikkanen and Rintamäki, 2019). Therefore, the term 'dark phase' is inappropriate; Buchanan (2016) has proposed the use of 'carbon reactions' for 'dark reactions'. Furthermore, the true 'light reactions' end after the primary charge separation steps in the RCs; both the electron transfer and the proton transfer reactions, in principle, can occur in darkness.

Cornelis B. van Niel (1931, 1941) showed that certain photosynthetic bacteria use H_2S instead of H_2O as an electron donor, producing sulfur instead of oxygen, and the global reaction of photosynthesis is:

$$2H_2A + CO_2 + \text{light energy} \rightarrow (CH_2O) + H_2O + 2A,$$

where A is sulfur in sulfur bacteria and oxygen in plants, algae and cyanobacteria. By analogy with photosynthetic bacteria, van Niel suggested that O_2 released by plants is derived from H_2O rather than CO_2. This was confirmed by Sam Ruben, Merle Randall, Martin Kamen and James Logan Hyde (see Ruben *et al.*, 1941), based on results using ^{18}O-labelled water.

Chlorophyll a fluorescence

As mentioned earlier, in addition to primary photochemistry, photosynthetic organisms lose some energy as heat (internal conversion) and as light (fluorescence). Fluorescence is radiative deactivation of (usually) the first singlet excited state of a molecule to the ground state. Kautsky and Hirsch (1931) discovered what others later called the 'Kautsky effect', which is Chl *a* fluorescence induction (ChlFI; see Govindjee, 1995). Kautsky and Hirsch observed (visually) transitory variations in Chl *a* fluorescence (ChlF) emitted by samples that were illuminated after a period of darkness; this ChlF has an increasing phase (peak, ~1 s) followed by a slower (5–10 min) decreasing phase. McAlister and Myers (1940) made an important observation by showing an inverse relationship between ChlF emission and CO_2 uptake. These ChlF transients were then studied, among other places, in the Photosynthesis Laboratory at the University of Illinois, Urbana-Champaign (beginning in the 1950s; see Govindjee and Papageorgiou, 1971; Papageorgiou, 1975; Govindjee and Satoh, 1986; Papageorgiou *et al.*, 2007). Because ChlF has been shown to be directly or indirectly affected by complex physical and biochemical processes taking place during photosynthesis, analysis of ChlFI curves is of importance in photosynthesis research (see reviews by Krause and Weis, 1991; Lazár, 1999, 2015; Strasser *et al.*, 2004; Stirbet and Govindjee, 2011; Stirbet *et al.*, 2018).

Photosynthetic unit (antenna and reaction centres): excitation energy transfer

An essential concept related to the light phase of photosynthesis is 'photosynthetic unit'. It was developed based on the crucial discovery by Emerson and Arnold (1932*a*, *b*) that ~2400 Chl molecules cooperate to evolve one molecule of O_2, while the minimum quantum requirement for the evolution of one O_2 molecule was 8–10 (Emerson, 1958; for the history of this discovery, see Nickelsen and Govindjee, 2011; Nickelsen, 2016). Gaffron and Wohl (1936) suggested the existence of 'photosynthetic units', where light energy absorbed by any antenna molecule is transferred as excitation energy among the pigment molecules, until finally it is trapped with high efficiency by a limiting enzyme (a 'photoenzyme', as implied by Emerson and Arnold, 1932*b*), which is equivalent to what we now call reaction centre (RC), a term introduced by Duysens (1952). Here, the primary charge separation (i.e. photochemistry) takes place (see e.g. Myers, 1994; Govindjee and Krogmann, 2004).

Experimental evidence for excitation energy transfer (EET) between photosynthetic pigments was initially obtained by comparing action spectra of photosynthesis and of sensitized ChlF in green, brown and red algae (see chapters 10–12 in Rabinowitch and Govindjee, 1969). We now have much more detailed knowledge on the molecular mechanisms of electronic EET in antenna, as well as on exciton trapping by the RCs (e.g. Croce and van Amerongen, 2013; van Amerongen and Croce, 2013; Roden *et al.*, 2016; Mirkovic *et al.*, 2017; Chan *et al.*, 2018).

Taking things apart

Robert Hill (1937) found that the 'light phase' of photosynthesis can operate independently from the 'dark phase' (the carbon reaction phase), since isolated chloroplasts can evolve O_2 in the presence of artificial electron acceptors [this reaction is called the 'Hill-reaction' in honor of Robert (Robin) Hill], even in the absence of CO_2. This concept led to a 'modularization' in the study of photosynthesis (Nickelsen, 2016), since even if these two partial processes are interrelated, the tendency after 1940 was to investigate them separately. Note that Mehler (1951) had found that molecular oxygen is also a Hill electron acceptor, and this reaction, called the 'Mehler reaction', has been shown to play an important role in photoprotection of photosynthetic organisms (Miyake, 2010).

The carbon reactions

The long-lived form of radioactive carbon, ^{14}C, was discovered by Samuel Ruben and Martin Kamen (1941). This radioactive isotope was used to decipher the major pathway of CO_2 reduction by photosynthetic organisms, by Andrew Benson (who did most of the early pioneering work, using ^{14}C), Melvin Calvin, James A. Bassham and co-workers (see Calvin *et al.*, 1950; Calvin, 1989; Bassham, 2005; Benson, 2005). For example, they found that ribulose 1,5-bisphosphate (RuBP; a 5-C sugar) was the acceptor of CO_2; the first stable product of CO_2 reduction was 3-phosphoglyceraldehyde (G3P; a triose phosphate); and that there was a cycle to regenerate the RuBP. Melvin Calvin received the Nobel Prize in Chemistry in 1961 for these discoveries; we are of the opinion that Andrew Benson should have been a co-recepient.

Photophosphorylation

Daniel Arnon *et al.* (1954*a*, *b*) showed that isolated chloroplasts can produce ATP in light; in addition, they showed that intact isolated chloroplasts can even perform complete photosynthesis (i.e. CO_2 fixation). Furthermore, Allen *et al.* (1958) found that photophosphorylation can be 'cyclical' (i.e. ATP is produced when there is a cyclic ET, which was shown to involve cyclic electron flow around PSI via Cyt b_6/f, CEF-PSI), or when there is 'non-cyclic' [i.e. during linear electron flow (LEF) from PSII to PSI) (see also Arnon, 1984; Tagawa *et al.*, 1963). A third pathway, labelled as 'pseudo-cyclic photophosphorylation', was also established, in which molecular oxygen plays the role of a terminal electron acceptor (i.e. the Mehler reaction; Mehler, 1951; Heber, 2002). Furthermore, a coupling mechanism between ATP synthesis and the ET, also in chloroplasts, was demonstrated by Dave Krogmann, Mordhay Avron and André Jagendorf (see Krogmann *et al.*, 1959). Note that the chloroplast coupling factor (CF1) for photophosphorylation, today known as ATP synthase, was discovered by Avron (1963).

The two-light reaction and the two-pigment system concept

The idea of two light reactions and two types of PSs had its beginning in the 1943 experiments of Robert Emerson and Charleton Lewis on the 'red drop' in the action spectrum of the quantum yield of photosynthesis (Emerson and Lewis, 1943) and in the 1957 'Emerson enhancement' effect, that is when the rate of photosynthesis in two lights given together was higher than the sum of the rates of photosynthesis measured when the two lights were given separately (Emerson *et al.*, 1957; also see: Govindjee and Rabinowitch, 1960); this discovery led to the well-known 'Z'-scheme of photosynthesis (Hill and Bendall, 1960; for the evolution of the Z-scheme, see Govindjee *et al.*, 2017). The very first Chl electron donors in the two PSs are P700 for PSI (identified also by an absorbance change around 705 nm; see Kok, 1956; Govindjee and Renger, 1993), and P680 in PSII, first suggested by Krey and Govindjee (1964) and shown to exist by Döring *et al.* (1969). Key experiments proving the Z-scheme were provided by Duysens *et al.* (1961) on the red alga *Porphyridium cruentum*, who showed the antagonistic effect of light 1 and light 2 on the redox state of cytochrome (Cyt). (Here, light absorbed by PSI was ~680 nm, and that absorbed by PSII was ~562 nm.) Furthermore, based on flashing light experiments, Witt *et al.* (1961*a*, *b*) provided evidence for the kinetics and on the existence of other intermediate steps in the Z-scheme; details of the ET components involved in the photosynthetic electron transport chain (PETC) are given in Fig. 1. However, of course, the physical confirmation for the existence and organization of the two PSs was the isolation and characterization via X-ray crystallography of the high-resolution spatial structure of PSII (e.g. Zouni *et al.*, 2001) and PSI (e.g. Jordan *et al.*, 2001).

Evidence from Chl a fluorescence measurements

Additional evidence for the two-pigment-system/two-light-reaction scheme in oxygenic photosynthesis was obtained by Govindjee *et al.* (1960) on *Chlorella* cells, using ChlF measurements. They showed an antagonistic effect of light 1 (i.e. predominantly absorbed by PSI) and light 2 (i.e. predominantly absorbed by PSII) on ChlF: addition of far-red light (light 1) to a shorter wavelength light (light 2) caused a decline (rather than an enhancement) of ChlF yield, compared to that produced by the two beams separately. As an explanation of this effect, Duysens and Sweers (1963) proposed that light 2 reduces a quencher Q, while light 1 oxidizes Q^- back to Q. The quencher theory of Duysens and Sweers was based not only on ChlF data published by Govindjee *et al.* (1960), but also by Butler (1962), who showed that variable fluorescence is mostly from PSII, and

far-red light, absorbed by PSI, gives a smaller amount of PSI fluorescence. The quencher Q (named X-320, but now labelled Q_A) was identified using single turnover flashes, and has an absorption spectrum with maximal spectral changes in the UV, at 270 and 320 nm (Stiehl and Witt, 1968). In several experimental studies (Stiehl and Witt, 1969; van Gorkom, 1974; see also Witt, 2004), plastoquinone difference spectra in the near UV (300–350 nm) were similar to light-minus-dark spectra of the first plastoquinone acceptor of PSII (i.e. $Q_A^{-\bullet} - Q_A$). According to Duysens and Sweers (1963), ChlF is proportional to the fraction of the reduced quencher ($[Q_A^-]/[Q_A]_{total}$; see a discussion in Stirbet and Govindjee, 2012; for other views see, Schansker *et al.*, 2011, 2014; Magyar *et al.*, 2018). Later, it was shown that several non-photochemical quenching (NPQ) processes take place in parallel with the photochemical quenching (i.e. by Q_A) during the so-called slow (~10 min) phase of the ChlF transient, and the proportionality of the fluorescence yield with $[Q_A^-]/[Q_A]_{total}$, observed during the initial (<1 s) Chl fluorescence rise, is lost (see below the section On NPQ of the excited state of Chl). Real advances in the study of these NPQ processes became possible only after Ulrich Schreiber developed a pulse-amplitude modulated (PAM) fluorescence instrument (Walz, Effeltrich, Germany) that could be used on leaves in the presence or the absence of actinic light (Schreiber, 1986; Schreiber *et al.*, 1986).

Vredenberg and Duysens (1963) observed that closure of RCs is accompanied by an increase in fluorescence yield of bacteriochlorophyll in *Rhodospirillum rubrum*, a purple anoxygenic photosynthetic bacterium, and concluded that several RCs share the same antenna. In an oxygenic photosynthesizer, the green alga *Chlorella*, Anne and Pierre Joliot (Joliot and Joliot, 1964) measured the rate of steady-state oxygen evolution, and correlated it with the fraction of active PSIIs (see also Joliot and Joliot, 2003). Joliot and Joliot (1964) observed that both the oxygen yield and the fluorescence yield are related, in a hyperbolic manner, to the fraction of closed PSII centres; this suggested that there is an energetic connectivity within PSIIs, that is an excitation visiting a closed PSII (i.e. with Q_A reduced) is redirected to another PSII. In this manner, the trapping cross-section of the open PSIIs increases as their neighbouring PSIIs become closed (see a review on PSII excitonic connectivity by Stirbet, 2013). Joliot and Joliot (1964) also derived theoretical equations describing the dependence of the ChlF yield (Φ_F) and the photochemical yield (Φ_P) on the fraction of open PSIIs, which included a connectivity parameter (p) for the probability of excitation energy transfer from a closed PSII to a neighbouring PSII (either closed or open). This was followed by publication of detailed papers on PSII excitonic connectivity by Paillotin (1976), Strasser (1978) and Butler (1980), the last two describing the process, using bipartite and tripartite PSII models of Butler and co-workers (Butler and Kitajima, 1975; Butler and Strasser, 1977). Later, Lavergne and Trissl (1995) and Trissl and Lavergne (1995) extended the concept of PSII excitonic connectivity, using an exciton–radical pair equilibrium model. The latter is equivalent to the reversible radical pair (RRP) model of Schatz *et al.* (1988); it assumes rapid exciton equilibration between all PSII pigments, including P680, and describes primary photochemistry (charge separation, recombination and stabilization) leading to closed PSII RCs. The major feature of the RRP model is *equilibrium*, i.e. reversibility of charge separation, meaning fast charge separation followed by fast charge recombination, in both the open and the closed PSII centres (see Fig. 2).

ATP synthesis

Peter Mitchell (1961*a*, *b*) proposed a chemiosmotic theory for phosphorylation, which suggests that a 'proton motive force'

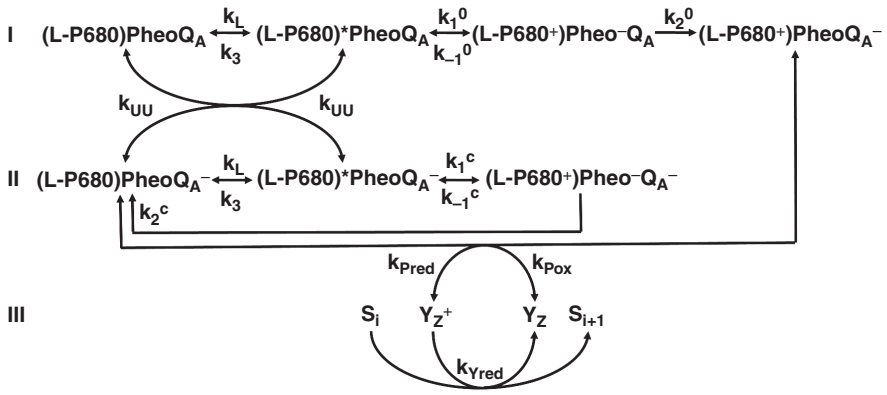

FIG. 2. Scheme showing the RRP (reversible radical pair) model and related reactions. The original RRP model is represented by the reactions on lines I and II, which are reactions occurring in an open PSII RC (when Q_A is initially oxidized) and a closed PSII RC (when Q_A is initially reduced), respectively. (L–P680)* denotes Chls in the light harvesting antenna of PSII (L) plus P680, which are in ultrafast excitation kinetic equilibrium, the asterisk (*) indicating the excited state. The rates constants are: k_L, overall rate constant of antenna excitation; k_3, overall rate constant of the excited state deactivation through heat dissipation and ChlF emission; k_1^o and k_1^c, rate constants of the primary charge separation in open and closed PSIIs, respectively; k_{-1}^o and k_{-1}^c, rate constants of the radiative (i.e. to the excited state) charge recombination between $P680^+$ and $Pheo^-$ in open and closed PSIIs, respectively; k_2^o, rate constant of charge stabilization in an open PSII, i.e. the ET from $Pheo^-$ to Q_A; k_2^c, rate constant of non-radiative (i.e. to the ground state) charge recombination between $P680^+$ and $Pheo^-$ in a closed PSII. The scheme presented here also includes excitation energy transfer (the energetic connectivity) between open and closed PSIIs (rate constant k_{UU}) and reversible reduction of $P680^+$ by Y_Z (rate constants k_{Pred} and k_{Pox}), as well as the reduction of Y_Z^+ by the manganese cluster of the oxygen-evolving complex (OEC; rate constant k_{Yred}), which produces an S-state transition from S_i to S_{i+1}, where S_i and S_{i+1} represent particular S-states. Modified from Lazár and Schansker (2009).

(*pmf*), i.e. the electrochemical potential of protons, couples the ET reactions with ATP synthesis (from ADP and inorganic phosphate, P_i). Mitchell received the Nobel Prize in Chemistry in 1978 for this hypothesis. Later, Paul Boyer and John E. Walker received the Nobel Prize in Chemistry in 1997 for their work on the structure of F1 mitochondrial ATPase and the mechanism of ATP synthesis (see e.g. Boyer, 2002). Hind and Jagendorf (1963) (see also Jagendorf and Uribe, 1966) showed how photosynthetic cells convert light energy into free energy stored in the ATP molecule on the basis of the chemiosmotic theory, particularly the ΔpH component. The *pmf* has two components, one due to the trans-thylakoid electric potential difference (i.e. the membrane potential, ΔΨ), and the other due to the trans-thylakoid difference in proton concentration (ΔpH), which builds up during water splitting reactions on the lumen side of PSII, and the translocation of stroma protons to the lumen during PQ pool reduction by PSII, and by Cyt b_6/f (including the Q-cycle; Mitchell, 1975) in relation to both the linear and the cyclic photosynthetic ET (see Fig. 1, and a historical review by Jagendorf, 2002). We remind the readers that just as André Jagendorf's work proved the importance of the ΔpH component (of *pmf*) for ATP synthesis, Wolfgang Junge's work proved the importance of ΔΨ in making ATP (see mini-review by Junge, 2004). However, a high ΔΨ component of the *pmf* was also shown to affect the equilibrium of redox reactions within PSII, and has been linked to higher rates of PSII charge recombination *in vivo*, and subsequent photodamage due to increased production of singlet oxygen (Davis *et al.*, 2016). On the other hand, low pH has been shown to inactivate oxygen evolution (Schlodder and Meyer, 1987); furthermore, release of Ca^{2+} from the oxygen evolving complex (OEC) has also been suggested to be the cause of this inactivation (Ono and Inoue, 1988; Krieger and Weis, 1993). For recent research (and reviews) on ΔΨ and ΔpH across the TM see, Strand and Kramer (2014), Kaňa and Govindjee (2016), and Lyu and Lazár (2017*a*, *b*).

Oxygen evolution

The key experiments that preceded the discovery of the water splitting mechanism, leading to O_2 evolution and $P680^+$ reduction in PSII, were done by Pierre Joliot and co-workers (Joliot, 1965; Joliot *et al.*, 1969). Joliot *et al.* (1969) discovered period 4 oscillations in oxygen evolution in algal suspensions when they were exposed to a sequence of single turnover (ST) saturating light flashes. These results were explained by Bessel Kok *et al.* (1970), who proposed a model (now known as Kok's oxygen clock model, or the Kok–Joliot model to many), in which the formation of oxygen requires sequential accumulation of four positive charges on the OEC, which cycles through five redox states, labelled as S_0, S_1, S_2, S_3 and S_4 (see Fig. 3). For the history of this discovery, see Renger and Govindjee (1993) and Joliot (2003). The first evidence for the participation of Mn in the S-states was obtained by Chuck Dismukes and Yona Siderer (1980), who obtained electron paramagnetic resonance (EPR) signals for the same. For a review on the functioning of the OEC, see Najafpour *et al.* (2012). For a recent review on oxygen evolution, see Lubitz *et al.* (2019).

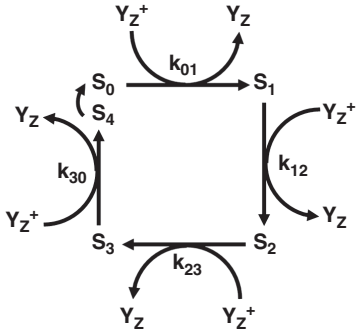

Fig. 3. Highly simplified scheme of Kok's oxygen clock model; misses and double hits are not shown. S_i (i = 0, 1, 2, 3, 4) represent the particular S-states of the manganese cluster of OEC. The S_4-state is assumed to be kinetically indistinguishable from the S_0-state. During an S-state transition, Y_Z^+ (formed through PSII reactions) is reduced (with rate constants k_{01}, k_{12}, k_{23} and k_{30}). Modified from Lazár and Schansker (2009). For a review, including the involvement of manganese, see Najafpour *et al.* (2012).

Mechanistic models for early events in photosynthesis

Bay and Pearlstein (1963) provided one of the first mathematical models of the exciton kinetics and trapping in a photosynthetic system; it was based on electronic excitation transfer, FRET (Förster resonance energy transfer; see Förster 1946, 1948; also see a historical review by Clegg, 2006). According to this model, the electronic excitation energy moves in a so-called 'random walk', hopping from one Chl to another Chl in the antenna, until it is trapped by an RC, or is dissipated as heat or fluorescence (also see: Govindjee, 2004). Starting from FRET, other more complex and elegant theories have now been developed to characterize the exciton dynamics in antenna (e.g. Engel *et al.*, 2007; Ishizaki and Fleming, 2009; Clegg *et al.*, 2010; Fassioli *et al.*, 2014).

On 'state transition' for regulation of balanced excitation in the two photosystems

State transition, a light-adaptive phenomenon that optimizes photosynthesis by synchronizing the turnover rates of PSII RCs and of PSI RCs, when there is an excitation imbalance between their antenna, was discovered by Cecilia Bonaventura and Jack Myers (1969) in *Chlorella* and, independently, by Norio Murata (1969*a*, *b*) in the red alga *Porphyridium cruentum* and spinach chloroplasts. The equilibration of PSII and PSI activities takes place through adjustment of the relative size of their antenna: During a transition from 'state 1' to 'state 2', the absorption cross-section (CS) of PSII antenna (which provides information on the PSII-specific rates of light absorption and represents an 'apparent' measure of PSII antenna size *in situ*, in units of $Å^2$ per PSII centre; see Osmond *et al.*, 2017) decreases and that of PSI antenna increases, while the opposite occurs during transition from 'state 2' to 'state 1'. The result is: the overall ChlF yield decreases in 'state 2' and increases in 'state 1', because, at room temperature, PSI has a much lower ChlF yield than PSII (Butler, 1962). State transitions have been shown by John Allen and collaborators to be regulated by the redox state of the PQ pool (Allen *et al.*, 1981; see Allen, 2002): the transition from 'state 1' to 'state

2' is triggered by the reduction of the PQ pool, and the transition from 'state 2' to 'state 1' is triggered by the oxidation of the PQ pool. In plants and algae, the controlling events take place at the Qp site of Cyt b_6/f (i.e. the binding site of PQH_2; see Zito *et al.*, 1999), where the PQ redox-state is sensed, which triggers the activation or inactivation of a protein kinase (Allen *et al.*, 1981): PQ pool reduction activates the protein kinase, and thus induces phosphorylation of mobile light harvesting complex (LHC) II, followed by its attachment to PSI antenna, while PQ pool oxidation inhibits the protein kinase, followed by dephosphorylation of the mobile LHCIIs by a phosphatase, and their re-attachment to PSII antenna (see Fig. 4 and reviews by Papageorgiou and Govindjee, 2011; Rochaix, 2014). For background on PSII, see Wydrzynski and Satoh (2005), on PSI, see Golbeck (2006), and on the Cyt b6f complex, see Cramer and Kallas (2016). Note that extensive dynamic changes in the organization and structure of the TMs are associated with state transitions, which include PSII antenna dissociation after LHCII phosphorylation by Stt7/STN7 kinases, or association with PSII after dephosphorylation by PPHI/TAP38 phosphatases (see above, and Iwai *et al.*, 2010). However, new research suggests that these protein kinases and phosphatases can also affect the likelihood of cyclic ET around PSI (see Wood *et al.*, 2019). On the other hand, Pribil *et al.* (2018) have shown that the changes in the shape of grana stacks are mediated by the CURVATURE THYLAKOID1 (CURT1) protein complexes, which were shown to facilitate adjustments in membrane curvature at the grana margins in a dose-dependent manner.

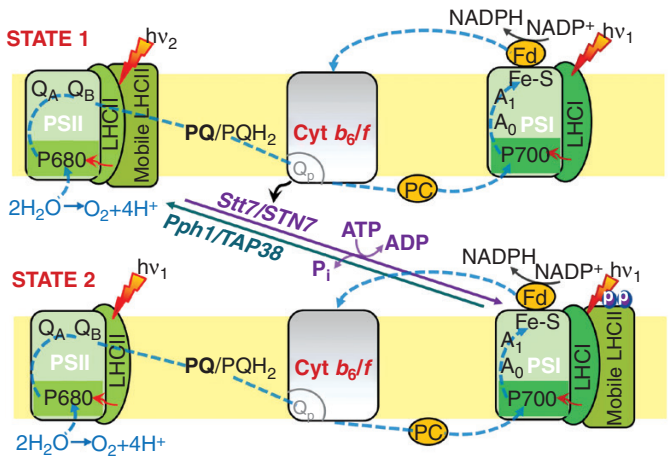

FIG. 4. Diagram of the mechanism of state transitions in plants and algae. In the diagram, the system is shown to be initially in 'state 1', with the absorption cross section (CS) of photosystem (PS) II being larger than that of PSI (it will have high Chl fluorescence yield because Chl in PSII is much more fluorescent than in PSI). During illumination, the plastoquinone (PQ) pool will be reduced by PSII because of higher absorption there. This is sensed by the Cyt b_6/f (via its PQH_2-oxidizing site, Q_p), and leads to activation of a kinase (*Stt7/STN7*) and phosphorylation of the mobile light harvesting complexes of PSII (LHCII), which then associate with the PSI antenna. The reverse occurs when the system is in 'state 2' initially, with the absorption CS of PSI being larger than that of PSII. Here, oxidation of the PQ pool by PSI during illumination will be sensed by the Cyt b_6/f, which leads to the inactivation of kinases, followed by de-phosphorylation of the mobile LHCIIs (by the phosphatases *Pph1/TAB38*) and their relocation to PSII. Abbreviations: A_0 and A_1, a particular Chl *a* molecule and a vitamin K1 molecule, respectively; Fe-S, three non-haem (heme) iron–sulfur centres; Fd, ferredoxin; Q_A and Q_B, plastoquinone electron acceptors of PSII; $NADP^+$ and NADPH, nicotinamide adenine dinucleotide phosphate in oxidized and reduced state; P680 and P700, reaction centre chlorophylls/primary electron donors of PSII and PSI; PC, plastocyanin. Figure modified from Allen (2003) and Rochaix (2014).

Two-electron gate on the electron acceptor side of PSII, and the requirement of bicarbonate

Bernadette Bouges-Bocquet (1973) and Bruno Velthuys and Jan Amesz (1974) independently discovered the two-electron gate (TEG) mechanism on the electron acceptor side of PSII in plants; it describes ET from Q_A to Q_B (see also Robinson and Crofts, 1983). As mentioned above, both Q_A and Q_B are PQs, but Q_A is a one-electron acceptor, and is permanently bound to the D2 protein of PSII. By contrast, Q_B is a two-electron acceptor that is bound to the D1 protein of PSII; it is strongly bound only when it is in Q_B^--state, but is weakly bound in its fully oxidized state (Q_B), and very weakly bound when in the fully reduced state (Q_BH_2). Following the primary charge separation: (1) Q_A is reduced to Q_A^- (via pheophytin, Pheo; discovered by Vyacheslav Klimov *et al.*, 1977); (2) Q_A^- then reduces Q_B to Q_B^-, and the latter remains tightly bound to D1; (3) after another light reaction, Q_B^- is then further reduced by Q_A^-, becoming fully reduced to Q_BH_2 (PQH_2), after the addition of two protons; and finally (4) because Q_BH_2 is loosely bound to D1, it is released in the membrane and replaced by another PQ molecule from the PQ pool (see Fig. 5, and reviews discussing light-induced PQ pool reduction by PSII by Cardona *et al.*, 2012; Müh *et al.*, 2012). A bicarbonate ion has been shown to have a very important role in the functioning of the TEG and Q_BH_2 formation (Wydrzynski and Govindjee, 1975; see reviews by Govindjee and van Rensen, 1978; van Rensen, 2002; Shevela *et al.*, 2012). A similar TEG was also discovered in bacteria, independently by Colin Wraight and André Vermeglio (see Vermeglio, 2002), but there is no bicarbonate effect there (see Wang *et al.*, 1992, and references therein). Note that the TEG model, the Kok model and the RRP model are important partial models that are used in more complex (or complete) models describing the photosynthetic ET (e.g. Nedbal *et al.*, 2009).

On NPQ of the excited state of Chl

In general, NPQ processes can be defined as processes that decrease ChlF through mechanisms other than photochemical quenching (i.e. Q_A quenching; e.g. Müller *et al.*, 2001; for a time line, see Papageorgiou and Govindjee, 2014). In this sense, the avoidance movement of chloroplasts in the leaf under high light conditions (i.e. qM; Dall'Osto *et al.*, 2014; Baránková *et al.*, 2016; Semer *et al.*, 2018, 2019), the state 1 to state 2 transition (qT_{12}; see above), as well as the photoinhibition (qI), initiated by the photodamage of PSII (Tyystjärvi *et al.*, 2005; Murata *et al.*, 2012; Tyystjärvi, 2013), would all be considered to be NPQ processes. However, according to Papageorgiou and Govindjee (2014), it is preferable to consider as NPQ processes only those in which the excess energy accumulated as singlet excited Chl *a* (^{1}Chl *a**) in PSII antenna is dissipated as heat (see Kitajima and Butler, 1975), such as the quickly

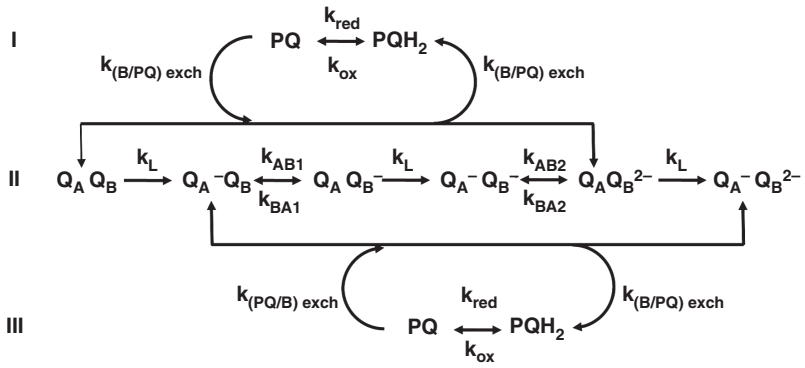

FIG. 5. Scheme of the two-electron gate (TEG) model and related reactions. The two-electron gate mechanism, by which electrons are transferred from Q_A to Q_B, is represented by the reactions on line II. The rate constants are: k_L, overall rate constant of Q_A reduction; k_{AB1} and k_{AB2}, rate constants of ET from the reduced Q_A to Q_B and Q_B^-, respectively; k_{BA1} and k_{BA2}, rate constants of backward ET from Q_B^- and Q_B^{2-} to Q_A, respectively. The reactions above and below line II describe the reversible exchange of doubly reduced Q_B (after its double protonation, which is implicitly assumed) with a PQ molecule from the PQ pool (rate constants $k_{(B/PQ)exch}$ and $k_{(PQ/B)exch}$); the reversible oxidation of the plastoquinol (rate constants k_{ox} and k_{red}) is implicitly assumed to be the result of chlororespiration and cyclical electron flow around PSI. Modified from Lazár and Schansker (2009).

reversible 'high-energy non-photochemical quenching' (qE), which develops in a few seconds and relaxes in 1–2 min (see Jahns and Holzwarth, 2012; and chapters in Demmig-Adams *et al.*, 2014), or other less clearly elucidated sustained forms of ChlF quenching processes (such as qH; Malnoë, 2018). This type of NPQ is induced by low lumen pH, being fully activated only after the *pmf* is established across the TM, when the TM is in a 'high-energy' state; it regulates the utilization of the light energy in PSII antenna in order to reduce photooxidative events that can damage the RCs. The exact relationship between lumen pH and NPQ is not fully understood; however, see discussions by Johnson (2011) and Zaks *et al.* (2013). There are three main requirements for qE activation: (1) a trans-thylakoid ΔpH formed in light (Wraight and Crofts, 1970; Briantais *et al.*, 1979); (2) the xanthophyll (VAZ) cycle, particularly the conversion of the carotenoid violaxanthin (V) to antheraxanthin (A) and zeaxanthin (Z) (Yamamoto *et al.*, 1962; Yamamoto and Higashi, 1978); and (3) the PSII protein subunit S (PsbS) (Li *et al.*, 2000; Brooks *et al.*, 2014). Barbara Demmig-Adams *et al.* (1989) (see also a historical review by Demmig-Adams, 2003) were the first to demonstrate that the extent of qE is proportional to the Z content of leaves; Demmig *et al.* (1987) further showed a correlation between Z and a form of qI manifested as a dark-sustained NPQ. Thus, they proposed that Z, which is derived from V in the xanthophyll cycle, is the link between the high energy state of the membrane and the heat dissipation of excess excitation energy of Chl *a* (see also Rees *et al.*, 1989, 1992). In the xanthophyll cycle, the content of V decreases during illumination and is restored in darkness: *Light*→V⇄A⇄Z⇐*Dark*. Violaxanthin deepoxidase (VDE) has a higher affinity for A than for V (Yamamoto and Higashi 1978), and binds on the lumen side of the membrane, at pH ≈ 5.0 (Hager and Holocher, 1994), which induces qE. Also, the NPQ kinetics was shown to depend on [Z], its induction being faster and its relaxation being slower when Z is present (see Johnson *et al.*, 2008). Adam Gilmore made an important contribution to the field, which included a successful collaboration with one of us (G) on the effects of intrathylakoid pH and VAZ cycle pigments on Chl *a* lifetime distributions and intensity in thylakoids (Gilmore *et al.*, 1995, 1998; Gilmore, 1997). On the other hand, the role of PsbS protein in qE is that of a pH sensor and quenching amplifier, as its amount in plant modulates the maximal qE level, but the underlying event is not yet fully understood (Horton *et al.*, 2008; Holzwarth *et al.*, 2009; Brooks *et al.*, 2014). However, there is also evidence that qE can be induced in the absence of PsbS (Johnson *et al.*, 2011), or even xanthophylls (Johnson *et al.*, 2012), if the lumenal pH is sufficiently low (i.e. lower than the value assumed by the 'moderate lumen pH paradigm'; see Kramer *et al.*, 1999). Finally, qE in algae is much more species-dependent than in plants. In unicellular green algae, or other algal groups (e.g. diatoms), the qE extent depends on the Light-Harvesting Complex Stress-Related (LHCSR) proteins (Peers *et al.*, 2009). In most organisms, the LHCSR level is strongly light-dependent, and in some species, such as *Chlamydomonas reinhardtii*, acclimation to low light leads to very low NPQ levels (Peers *et al.*, 2009).

Recently, Schreiber *et al.* (2019) have described a rapidly induced NPQ process during a pulse of high-light intensity in a dilute suspension of *Chlorella vulgaris*; they called this process HIQ [high (light) intensity quenching]. The amplitude of the HIQ increases linearly with the effective rate of quantum absorption by PSII, reaching ~8 % of F_M (i.e. the maximum Chl fluorescence measured in dark-adapted samples). This quenching rapidly relaxed after the pulse, and was shown to be caused by annihilation of ^{1}Chl* *a* by ^{3}Car* (excited state of a carotenoid in triplet state).

MODELLING CHL FLUORESCENCE INDUCTION IN PLANTS, ALGAE AND CYANOBACTERIA

ChlF emitted by plants and algae has little involvement in the process of photosynthesis, being one of the pathways in which excess excitation energy is dissipated by photosynthetic organisms. However, ChlFI kinetics is well recognized to have an intricate connection with many processes taking place during the

conversion of light energy into a stable chemical form. Because it is a non-destructive measurement, although indirect, the ChlFI has numerous applications in the study of photosynthesis (see chapters in Papageorgiou and Govindjee, 2004), while its modelling is a straightforward way to verify various theories regarding different photosynthetic processes. Note that ChlFI in cyanobacteria is in part affected in different ways by the activity of the photosynthetic apparatus than in plants and algae, and this is due to their structural differences (see Stirbet *et al.*, 2019), but its modelling is not described in this review.

The ChlFI curve has been labeled O-J-I-P-S-(M)-T, where O-J-I-P represents the first fast (<1 s) phase, also known as the fast ChlF rise, and P-S-(M)-T the slower (5–10 min) phase (see Fig. 6, and a review by Govindjee, 1995). Level O (origin) is the first measured minimum fluorescence level; J and I are intermediate inflections; P is the peak; S is the semi-steady state; M is a maximum, which, in plants, at room temperature is often seen only at low light intensities, but has been observed in *Arabidopsis thaliana* under low (freezing) temperature conditions (Mishra *et al.*, 2019); and T is a terminal steady state level.

The fast phase was labelled OIDP (Munday and Govindjee, 1969), as OI_1I_2P (Schreiber, 1986) and then OJIP (Strasser and Govindjee, 1991); the O-J-I-P curves are measured only under a high intensity of excitation light. At low light the J step is missing, so that only an O-I-P curve is observed (Strasser *et al.*, 1995; Tomek *et al.*, 2001). Below, we briefly discuss several models for the O-J-I-P fluorescence rise, as well as for the entire O-J-I-P-S-(M)-T transient or just the slow P-S-(M)-T phase (see also reviews by Lazár, 1999; Lazár and Schansker, 2009; Stirbet *et al.*, 2014).

Modelling strategy, definition of the Chl fluorescence signal, and some selected partial models of PSII

Mathematical modelling is an essential part of modern biology and can have several purposes. In any experimental study, the measured data provide information about how the explored system works, and based on these, we formulate hypotheses about how the explored system is functioning. By converting the hypotheses into a mathematical model, running the model and comparing the calculated results with experimental data, we can judge if the model describes the data well or not. In this case, the structure of the model (i.e. the hypotheses as such) and also the values of model parameters can cause agreement/disagreement between the results obtained with the model and the measured data. Regarding the values of the model parameters, we can run the model with fixed parameter values, taken from the literature, or we can fit the values to get the best agreement between the model results and experimental data. However, in the latter case, we may find a perfect agreement, but only by using unrealistic values of the model parameters (based on the literature), which usually rules out the correctness of the model. On the other hand, when values of system variables are not known from the litrrature and/or are not directly accessible from experiments, the fitting can provide this information, assuming the model structure is correct.

Furthermore, a so-called metabolic control analysis (MCA) can be performed, which quantifies the extent to which a given process (hypothesis) affects a given result (for a review see Visser and Heijnen, 2002). Sometimes, this quantification can be made easy only by using modelling rather than by doing experiments, because it is not always possible to infer the desired (initial) state of the experimental system, or to experimentally modify the parameters of the system, as needed to perform MCA.

Finally, if we have a robust model that describes well the various measured data, we can modify the model parameters and track the results, or in other words, we can perform 'experiments' without measuring anything – i.e. biological experiments *in silico*. These *in silico* experiments are very useful in making predictions that allow us to determine the role of model parameters, or to design experiments to prove or refute certain predictions. Concerning the modelling of ChlFI discussed below, it is important to keep in mind that a qualitative agreement between experiment and theory is a useful goal. The ChlFI is a manifestation of a very complex biological system, and therefore describing it correctly and comprehensively is difficult – this is quite different from modelling technical systems, which can be described correctly, and where a quantitative agreement between experiments and theory is strictly required.

Several approaches have been used for the formulation of a fast ChlF rise model, or for the entire ChlFI. The variable ChlF is emitted mostly from PSII (reviewed by Krause and Weis, 1991; Dau, 1994; Govindjee, 1995; Lazár, 1999, 2006; Stirbet and Govindjee, 2011, 2012). The basic strategy for modelling the fast ChlF rise has been to first use a model of the ET reactions occurring only in PSII, but then later add ET reactions beyond PSII, especially for the modelling of the entire ChlFI. The formulation of a ChlFI model also depends on the specific ET components considered, and then, on the way, the variable ChlF emitted during the transient is defined. The basic approach in the definition of the variable ChlF is based on the early work of Duysens and Sweers (1963) and the quencher theory defined there, later identified to be due to Q_A (see above the subsection Evidence from Chl *a* fluorescence measurements). According to this theory, if Q_A is oxidized, ChlF is low and if Q_A is reduced, ChlF is high, and the variable ChlF is proportional to

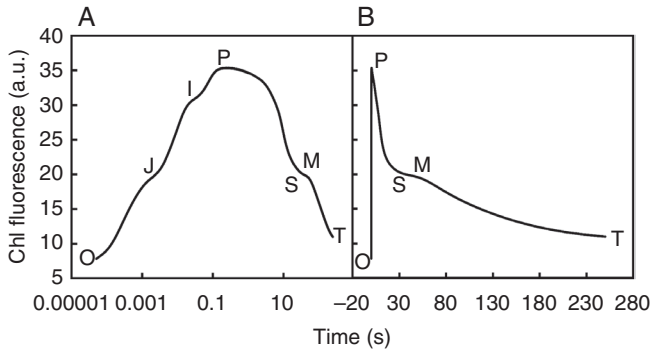

Fig. 6. Chlorophyll *a* fluorescence induction curves measured in leaves of 10-d-old barley (*Hordeum vulgare* L.) plants kept in darkness for 20 min before the measurement, shown on a logarithmic time scale (A), and on a linear time scale (B); a.u., arbitrary units. The O, J, I, P, S, M and T steps marked in the figure represent: O, the origin (minimum fluorescence F_O); J and I, intermediary fluorescence levels at 2 and 30 ms (F_J and F_I); P, the peak (F_P); S, a semi-steady state level; M, a maximum; and T, the terminal steady state. Measurements were made under continuous red (650 nm) light of 2500 µmol photons m^{-2} s^{-1} with a Plant Efficiency Analyser (Hansatech, UK). Modified from Stirbet *et al.* (2018).

the fraction of Q_A^-. Moreover, the energetic PSII connectivity (mentioned earlier) can be also considered in modelling the variable ChlF.

Taken together, the most basic approach used to model the fast ChlF rise has been to define a PSII model that describes the redox changes of Q_A during reduction of the PQ pool. These redox changes are modulated by Q_B, the second PQ electron acceptor of PSII, which unlike Q_A is a two-electron PQ acceptor of the PSII RC; originally, it came from the PQ pool, transiently binding to the Q_B-site. The reduction of Q_B to plastoquinol is described by the TEG model (Bouges-Bocquet, 1973; Velthuys and Amesz, 1974), which is the fundamental partial model used in ChlFI modelling (see discussion earlier, and Fig. 5). Thus, one group of models describing the fast ChlF rise, including the first ever models (see below the subsection Modelling the fast Chl fluorescence rise by using only models of PSII reactions), are based on the TEG model. The charge stabilization on Q_A (i.e. the reduction of Q_A by $Pheo^-$) means that the PSII RC is closed and thus the ChlF is high. However, this charge stabilization is preceded by the formation of $P680^+Pheo^-$ (see Fig. 2). Thus, when either $P680^+$ and/or $Pheo^-$ are present, the PSII RC is closed, but the ChlF decreases in their presence, as both $P680^+$ and $Pheo^-$ are quenchers of ChlF (for $P680^+$, see Okayama and Butler, 1972; Shinkarev and Govindjee, 1993; Steffen *et al*., 2001, 2005; for $Pheo^-$, see Klimov *et al.*, 1977). Quenching of Chl fluorescence by $P680^+$ accumulation has been considered in several models of the fast ChlF rise (e.g. Lazár, 2003; Laisk and Oja, 2018). Accumulation of reduced Pheo was shown to take place only under illumination at 200–220 K (Klimov *et al.*, 1980; Breton, 1982). Nonetheless, Vredenberg (2000, 2008, 2011) has assumed, in his O-J-I-P model, not only that $Pheo^-$ accumulates at room temperature, but also that ChlF is higher when both Q_A and Pheo are reduced than when only Q_A is reduced. Strasser and Stirbet (2001) have also simulated and fitted a fast ChlF rise with a simple TEG-based model, but considering three different PSII redox states that contribute to the fluorescence signal: (1) with Q_A^-; (2) with $Pheo^-$; and (3) with $PheoQ_A^-$ and $Pheo^-Q_A^-$; ChlF in the presence of $Pheo^-Q_A^-$ was considered to be two-fold larger than that when $PheoQ_A^-$ was present. The experimental O-J-I-P curve was fitted quite well by all three models, but the parameters of the models and the kinetics of the PSII redox states were different in each case. Thus, overparametrized models cannot be validated by fitting one experimental curve, and other approaches must be also used to reach firm conclusions. These can be, for example, measurements of the kinetics of the redox states of PSII during the ChlF transient, as well as through *in silico* experiments, in which the basic parameters of the model are kept constant.

On the other hand, ChlF yield during ChlFI has also been defined by using ratios of the rate constants related to fluorescence emission, heat dissipation and photochemistry (Goltsev and Yordanov, 1997; Laisk *et al.*, 2006; Ebenhöh *et al.*, 2014; Stirbet and Govindjee, 2016). A better estimation of the ChlF signal, in models used to simulate the ChlFI, is obtained by considering fluorescence as a radiative deactivation of the singlet excited state of Chl (i.e. ^{1}Chl*); this was used in the modelling of the fast ChlF rise by Baake and Schlöder (1992) (see also Lebedeva *et al.*, 2002; Lazár, 2003; Belyaeva, 2004). If the ChlF signal is defined by the redox states of Q_A or by the concentration of ^{1}Chl*, the model must include these entities. The reactions among the excited states of Chl *a* in PSII antenna that include P680 and Pheo, besides Q_A, have been described by the RRP model of Schatz *et al.* (1988); it was based on measurements of ChlF decay in the picosecond range after excitation by a short laser pulse. In the RRP model, charge separation between P680 and Pheo is reversible and is followed by charge stabilization (ET from $Pheo^-$ to Q_A) in the open PSII RCs, and by non-radiative charge recombination (to the ground state) in closed PSII RCs (see Fig. 2). Thus, the RRP model is the second fundamental partial model, in addition to the TEG model, which must be considered in modelling the ChlFI.

If the formation of $P680^+$ is considered in a model, then the reduction of $P680^+$ must be also included, i.e. reactions on the donor side of PSII, as well as the recombination reactions between $P680^+$ and $Pheo^-$ or Q_A^-. The $P680^+$ is reduced by tyrosine 161 (i.e. Y_Z; Debus *et al.*, 1988), which is, in turn, reduced by OEC. Electrons are donated to Y_Z^+, by OEC, as it undergoes the S-state cycle (Kok *et al.*, 1970; Fig. 3). Kok's model of OEC is the third fundamental partial model for the description of PSII function. This model also includes parameters called 'misses' (when the light flash used does not lead to an S-state advancement) and 'double hits' (when the flash leads to an advancement by two S-states). Kok's model has been modified by Jablonsky and Lazar (2008) by including the so-called intermediate S-states, which enable omission of the misses and double hits in the model.

Modelling of the fast Chl fluorescence rise measured after treatment with a herbicide

Because many photosynthetic processes affect ChlFI, herbicides that interrupt the ET from Q_A to Q_B have been used to simplify the observed curves. Note that many different herbicides are employed to kill weeds, and this can be achieved by using different substances that operate through various other mechanisms, but here we discuss only those that block the Q_B-pocket of PSII. DCMU (3-(3′,4′-dichlorophenyl)-1,1-dimethylurea) is a herbicide that has been frequently used in such studies; it binds to the Q_B-pocket, blocking ET beyond PSII (e.g. Oettmeier *et al.*, 1980), which leads to a faster closure of PSII RCs during illumination and to a faster accumulation of Q_A^-. Binding of DCMU at the Q_B-pocket results in a faster sigmoidal ChlF rise to its maximal value (F_M), which is reached approximately at the J step (~2 ms) of the ChlF rise, measured (under saturating light) with an untreated sample. The gradual binding of DCMU to the Q_B-pocket of PSII, and thus the gradual closure of PSII, as reflected in changes in the O-J-I-P transient, was modelled by Lazár *et al.* (1998). Here, the diffusion of DCMU was described using Fick's laws, and the reaction of DCMU at the Q_B-binding site of PSII, by second-order kinetics. From this work, Lazár *et al.* (1998) provided values of the diffusion coefficient of DCMU, and the second-order rate constant of DCMU binding to the Q_B-pocket of PSII.

The sigmoidal shape of the fast ChlF rise measured with DCMU has been suggested to reflect energetic connectivity (*p*) between the PSII units (Joliot and Joliot, 1964; also see above for discussion). This concept is tightly connected with a type of PSII

heterogeneity, namely PSII α/β antenna heterogeneity (Melis and Homann, 1975). The PSIIα units, the main PSIIs, have a large and energetically connected light-harvesting antenna. The size of the antenna is reflected in the rate constant of the fast ChlF rise, measured with DCMU, and PSII connectivity is reflected in the value of the parameter *p*; the PSIIβ units have smaller antenna and a lower energetic connectivity. Several different procedures have been used to obtain quantitative information on this PSII heterogeneity (see Hsu *et al.*, 1989). To increase the reliability and accuracy in the determination of PSII antenna heterogeneity, Lazár *et al.* (2001) have fitted the values of rate constants, the parameter *p* and the fractions of particular PSII types to several curves of fast ChlF rise in the presence of DCMU, measured at different light intensities, by using just one fitting procedure; results from this work were in good agreement with those in the literature.

The fast ChlF rise measured with DCMU has also been explored using the RRP model by Trissl *et al.* (1993), Lavergne and Trissl (1995), and Trissl and Lavergne (1995), with PSII energetic connectivity included. The RRP model has been further improved by Lazár and Pospíšil (1999) by the addition of $P680^+$ reduction step(s) on the (electron) donor side of PSII; for this, they had used the fast ChlF rise in the presence of DCMU measured at high temperatures. Decreases in PSII energetic connectivity and in the rate of $P680^+$ reduction by Y_Z were suggested to occur in the photosynthetic samples kept at high temperatures (e.g. 47 °C for 5 min; Guissé *et al.*, 1995; Srivastava *et al.*, 1997), but these conclusions were based on results on samples, without DCMU. By contrast, Lazár and Pospíšil (1999) have simulated the fast ChlF rise, in the presence of DCMU, at high temperatures by omitting PSII energetic connectivity, and by decreasing the rate constants related to the electron donation to $P680^+$.

To study photoinhibition in DCMU-treated samples, Vavilin *et al.* (1998) and Lazár *et al.* (2005) have simulated fast ChlF rise curves by using the RRP model. Lazár *et al.* (2005) further extended the RRP model by considering a possible protective function of Cyt b_{559} against photoinhibition, as proposed by Thompson and Brudvig (1988) and by Nedbal *et al.* (1992). Cyt b_{559} is indeed reduced by $Pheo^-$, which then donates electrons to $P680^+$, involving a CEF around PSII. However, an argument against such an ET may be in the crystal structure of PSII (e.g. Zouni *et al.*, 2001; Kamiya and Shen, 2003), which shows that the distance from the Pheo in the active D1 branch of PSII and the Cyt b_{559} is too long (~45 Å) to allow an ET between them. However, the distance between Pheo in the inactive D2 branch of PSII and the Cyt b_{559} is shorter (22 Å), and ET by tunnelling has been reported for such distances (Page *et al.*, 1999). Thus, the Pheo in the model of Lazár *et al.* (2005) could be Pheo in the D2 branch of PSII.

Modelling the fast Chl fluorescence rise by using only models of PSII reactions

Mathematical analyses of the fast ChlF rise were published in the 1960s (Malkin and Kok, 1966; Malkin, 1966; Munday and Govindjee 1969). Munday and Govindjee (1969) measured the O-I-D-P (where D is for a dip) ChlF rise curve in *Chlorella pyrenoidosa* and related it successfully to variations in the fraction of reduced Q_A. In their paper, the dip was analysed by studying the transient oxidation of Q_A^- by PSI.

In all likelihood, the first 'real' model of the fast ChlF rise [i.e. a scheme of ET reactions and a related set of coupled ordinary differential equations (ODEs)] was that of Holzapfel and Bauer (1975). This model was rather complex: it described the complete ET chain in the TM, including the formation of NADPH and ATP. On the other hand, some details of the photosynthetic ET were not included in the model, due to limited knowledge of the photosynthesis process at that time. In this model, the ChlF was assumed to be proportional to the amount of Q_A^-. Holzapfel and Bauer (1975) were able to qualitatively simulate the rate of oxygen evolution at different light intensities, the fast ChlF rise of control samples, and of those treated with DCMU and/or 2,5-dibromo-3-methyl-6-isopropyl-p-benzoquinone (DBMIB, which blocks the electron flow between PQ and Cyt b_6/f; cf. Trebst and Reimer, 1973), as well as of samples that were dark-adapted under anaerobic conditions. This model was further used by Holzapfel (1978), where the effect of $\Delta\Psi$ across the TM was included. It is unclear why these models were missed by others. However, several models on the fast O-I-P ChlF rise, measured using light intensities lower than 1200 µmol photons m^{-2} s^{-1}, are available (Renger and Schulze, 1985; Hsu, 1992*a*, *b*; Goltsev and Yordanov, 1997; Tomek *et al.*, 2003); these models were based on the TEG model, where ChlF signal was assumed to be proportional to the amount of reduced Q_A (for an exception, see Goltsev and Yotdanov, 1997). Tomek *et al.* (2003) have further used the amplitude of the I step to estimate the fraction of 'Q_B-non-reducing centres' (i.e. PSIIs which cannot reduce Q_B).

Different TEG models, and PSII redox states with reduced Q_A to calculate the ChlF signal, were also used in modelling the O-J-I-P ChlF rise measured under saturating light (~3000 µmol photons m^{-2} s^{-1}; Stirbet and Strasser, 1995, 1996; Lazár *et al.*, 1997; Stirbet *et al.*, 1998, 2001; Strasser and Stirbet, 2001; Tomek *et al.*, 2001; Sušila *et al.*, 2004). In these studies, the authors mainly showed how selected parameters of the models (e.g. initial concentrations and values of the rate constants) affect the shape of the O-J-I-P curves. However, Stirbet and Strasser (1996) showed that consideration of second-order kinetics for the reactions between Q_A and Q_B in the TEG model gives different simulated O-J-I-P curves compared to those obtained in the simulation where first-order kinetics is used. Strasser and Stirbet (1998) have also simulated O-J-I-P ChlF transients with a TEG model, by taking into account the heterogeneity of the PSII population in relation to PSII antenna, PSII energetic connectivity, and the ability of PSII to reduce Q_B ('Q_B-reducing' vs. 'Q_B-non-reducing' RCs).

Sušila *et al.* (2004) considered a hypothetical sample divided into ten layers of the same thickness, and calculated the light intensity in each layer, based on the Lambert–Beer attenuation law, in order to determine the light gradient inside the sample. They then simulated the fast ChlF rise curve for each layer, by using the same model as in Lazár *et al.* (1997) and Tomek *et al.* (2001), and summed the ChlF signal from all the layers to obtain the total ChlF signal. Their results showed that the light gradient inside a sample can significantly affect the shape of the fast ChlF transient. We note that in all the above models for the O-J-I-P ChlF rise, with the exception of those used by Stirbet *et al.* (1998, 2001) and Strasser and Stirbet (1998, 2001), the presence of an unknown component X that accepts electrons from the Q_B^- was assumed to exist.

Guo and Tan (2011) have extended the TEG model by taking in account the existence of a light-harvesting antenna system. Later, Feng *et al.* (2018) extended the above model by including the pH-dependent NPQ process, which allows the fitting of the decrease of the ChlF signal from the peak 'P' to 'S' and/or the 'T' level. To fit the O-J-I-P ChlF curves measured at different temperatures (20, 25, 30 °C), the rate constants in the model of Guo and Tan (2011) were assumed to be dependent on the temperature according to the Arrhenius law (Xia *et al.*, 2018). Because the formation of ^{1}Chl* during illumination was included in the models used in all three studies above, the ChlF signal was defined as radiative deactivation of ^{1}Chl* in the PSII antenna.

In some of the models just mentioned, the function of the PSII donor side was implicitly included. By contrast, in the models of Stirbet *et al.* (1998, 2001), Chernev *et al.* (2006), Lazár and Jablonský (2009), and Laisk and Oja (2018), the function of the PSII donor side was included explicitly, and that too in combination with the TEG model. Stirbet *et al.* (1998, 2001) not only included the S-states of OEC, but also the PSII energetic connectivity, and the quenching of the ChlF signal by $P680^+$ and by the oxidized PQ molecules. Stirbet *et al.* (1998, 2001) then simulated (or fitted) the O-J-I-P ChlF transient by defining the ChlF signal to be proportional to the amount of reduced Q_A, and by considering different initial fractions of Q_B and Q_B^-, or of the S_1 and S_0 states of OEC. In the model of Lazár and Jablonský (2009), all the S-state transitions of OEC were taken into account, as well as the redox states of $P680^+$ that were explicitly considered in combination with the TEG model, which was then used for simulation of the O-J-I-P ChlF transient. In their study, the effect on the simulated fast ChlF curve was described by using (1) first- or second-order reaction kinetics for electron donation from the OEC to $P680^+$; (2) one second-order reaction or two subsequent reactions for the Q_B^{2-}/PQ exchange; and (3) all possible reactions between the ET components, or of fewer 'logical' reactions.

Other models used for simulation of the fast ChlF rise are those that include, in addition to the TEG model, the description of the fast events in the PSII RC (i.e. charge separation, recombination and stabilization) described by the RRP model. Models by Baake and Schlőder (1992) and Belyaeva *et al.* (2011) belong to this group, where reduction of $P680^+$ by Y_Z (via OEC) was implicitly included. Other authors (Lazár, 2003; Zhu *et al.*, 2005; Matsuoka *et al.*, 2015) have explicitly included Y_Z and the S-state transitions of OEC.

Lazár (2003) provided a detailed analysis of how values of particular rate constants and initial conditions affect the simulated fast O-J-I-P ChlF curves. An important aspect of the ChlFI curves analysed by simulations in this work is the origin of the minimal ChlF level (F_O) which is the initial ChlF, when all PSII RCs have all Q_A in the oxidized state; F_O originates from the radiative deactivation of the excited PSII state [(antenna-P680)*PheoQ$_A$Q$_B$; see Fig. 7]. Interestingly, although the model of Lazár (2003) is one of the most detailed models of PSII reactions (consisting of a set of 44 coupled ODEs), yet it was not able to simulate typical O-J-I-P ChlF transients, as the ChlF signal increased from the J step to a maximum, which was reached at the I step position in the experimental curves (Fig. 7).

The inability to simulate the proper time-dependence of the ChlF signal by the detailed model based only on PSII redox states is one of the arguments that a proper model for the O-J-I-P ChlF rise should also describe ET reactions occurring beyond the PQ pool, as already inferred by Munday and Govindjee (1969) and later confirmed in other studies (i.e. Schreiber *et al.*, 1989; Schansker *et al.*, 2003, 2005).

Modelling the fast Chl a fluorescence rise with models that consider electron transport in and around the TM

The last group of models used in simulation of the O-J-I-P ChlF transients are those that include ET reactions occurring in and around the TM (Lebedeva *et al.*, 2002; Kroon and Thoms, 2006; Lazár, 2009; Makarov *et al.*, 2012; Belyaeva *et al.*, 2016, 2019), or even the metabolic reactions in the stroma (e.g. the Calvin–Benson cycle; see Laisk *et al.*, 2006, 2009; Zhu *et al.*, 2013). Given the all-inclusive nature of these models, some of them were also used for modelling of the the entire ChlFI (see below). A diagram of the reactions considered in the model proposed by Lazár (2009) is shown in Fig. 8. This model consists of a set of 42 coupled ODEs, and the ChlF emission is defined as being proportional to the amount of reduced Q_A. In addition, the ΔA_{820} signal, describing redox changes of P700 and plastocyanin (PC), was also modelled. To show that the ET reactions beyond the PQ pool affect the shape of the simulated fast ChlF transients, Lazár (2009) also analysed *in silico* the effects of DBMIB and MV [methylviologen, which accepts electrons from both the iron–sulfur cluster of PSI and ferredoxin (Fd); Sétif, 2015]. The shapes of the simulated fast ChlF transients and of ΔA_{820} signal were qualitatively in agreement with the experimental curves (see Fig. 8). This model is also a part of e-photosynthesis.org (Šafránek *et al.*, 2011), which is a web-based platform for modelling complex photosynthetic processes.

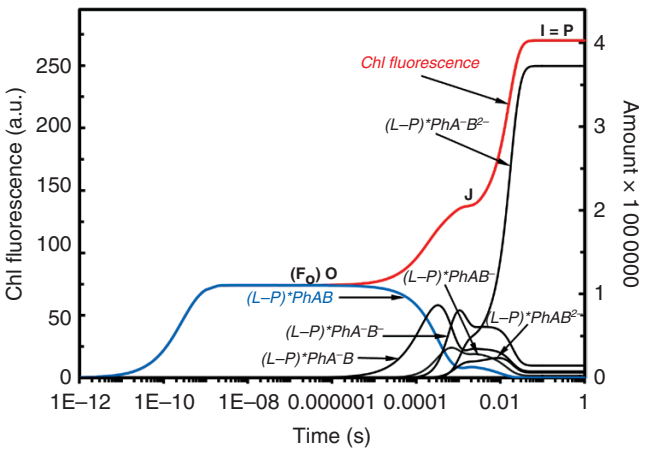

FIG. 7. Simulations of the O-J-I(=P) ChlF rise (see text) and of the model forms of photosystem (PS) II in the excited state, which mainly contribute to the (chlorophyll *a*) fluorescence transient, are shown on a logarithmic time scale. Abbreviations: (L-P)*, the excited state of the PSII antenna, which is equilibrated among all light harvesting Chls, including P680; Ph, pheophytin; A and B, the first and second plastoquinone acceptors of PSII (Q_A and Q_B). The time course of the PSII model form (L-P)*PhAB at the beginning of the transient, which represents excited open PSII RCs (i.e. with oxidized Q_A), is at the origin of the minimal ChlF, F_O. Modified from Lazár (2003).

In all the models mentioned above, the variable ChlF signal was assumed to originate from the PSII antenna. The problem with direct measurement of the variable ChlF from PSI *in vivo* (not from isolated PSI complexes) is that it overlaps spectrally with the PSII ChlF. However, some experimental results, presented in the literature (see Lazár, 2013), show the existence of a variable ChlF originating in PSI, at least under certain conditions. Lazár (2013) presented a very detailed model of the ET reactions in PSI (i.e. a set of 106 coupled ODEs), and simulated fast ChlF transients originating only from PSI. The ChlF signal was defined as the radiative deactivation of ^{1}Chl*. PSI was further shown to emit variable ChlF, and its contribution to the total maximal variable ChlF signal from the two PSI and PSII was ~8–17 % (Lazár, 2013). Future studies are needed to quantitatively assess these findings.

Rule-based modelling of the fast Chl fluorescence rise

All the models of the fast ChlF rise discussed thus far have described the photosynthetic processes by using sets of coupled ODEs. Each ODE was used to describe the time-change of a particular PSII redox form (i.e. state variable) of the model. This approach is deterministic, because in any run of the model, the same solution is obtained.

If too many state variables (coupled ODEs) are considered in a model, it becomes difficult to obtain model results, due to high requirements of computational time and hardware; this is because all ODEs must be solved simultaneously at each time of system evolution. While there are ways (specific for each model) to decrease the number of equations, this problem can be better overcome by employing a rule-based modelling approach, where rules are defined that are equivalent to the particular ET reactions. Furthermore, random numbers are generated, and these determine (using internal decision process) which rules should be considered in each particular step of the model run, i.e. in each 'evolvement' of the system in time. Thus, a time course of the system behaviour would be described by a sequence of particular rules, which are slightly different in different model runs, i.e. small differences between solutions are obtained after different runs of the model. Thus, this approach would be stochastic (i.e. random). The rule-based

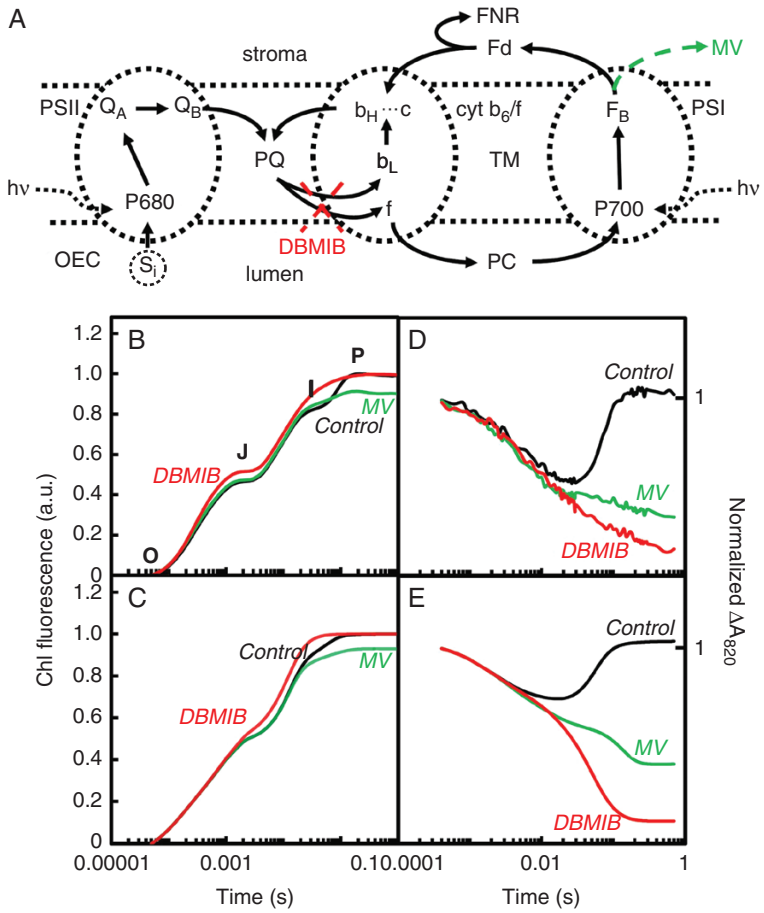

FIG. 8. Diagram of the ET reactions used in the model of Lazár (2009) (A), the O-J-I-P ChlF transients measured on control (= untreated) leaves, as well as on leaves treated with 2,5-dibromo-3-methyl-6-isopropyl-p-benzoquinone (DBMIB, which inhibits ET in the cytochrome b_6/f, see A) or with methyl-viologen (MV, which accepts electrons from the iron–sulfur cluster of PSI and ferredoxin, Fd, see A) (B), and the respective curves simulated with the model (C), the ΔA_{820} curves measured under the same conditions (D), and the respective curves simulated by the model (E). The curves are shown on a logarithmic time scale. Abbreviations: S_i, the S-states of the oxygen-evolving complex (OEC); f, b_L, b_H···c, cytochrome f, low/potential cytochrome b_6, and high-potential cytochrome b_6 in kinetic equilibrium with the haem c of cytochrome b_6/f complex; PC, plastocyanin. Modified from Lazár (2009).

stochastic approach by means of kinetic Monte Carlo simulations has been applied for modelling of the O-J-I-P ChlF transient by Xin *et al.* (2013), Guo and Tan (2014), Maslakov *et al.* (2016) and Antal *et al.* (2018). However, in all these cases, the shapes of simulated ChlFI curves were the same (except for the noise) as when using the deterministic approach. Similarly, the O-J-I-P curve was also simulated using stochastic π-calculus (Tokarčík, 2012) and rule-based language-simplified Kappa (Nižnan, 2014). Much further work is needed to obtain conclusive results from this approach.

Modelling the slow PS(M)T phase of the Chl a fluorescence induction curve

The nomenclature of P-S-(M)-T for the slow phase of the ChlFI was first used by Papageorgiou and Govindjee (1968*a*, *b*). Compared with the fast ChlF rise, this phase is much more complex and less well understood, as the fluorescence yield is modulated by an increasing number of processes triggered during this phase, besides the photochemical quenching by Q_A (see above), such as: (1) the NPQ of excited singlet ^{1}Chl* *a* in PSII antenna, induced by low pH in the lumen (i.e. the high-energy NPQ qE; Horton *et al.*, 1996; Rochaix, 2014); (2) state transitions (i.e. qT_{12} or qT_{21}) that regulate the absorption CS of PSI and PSII (with 'state 1' being more fluorescent than 'state 2'; see Papageorgiou and Govindjee, 2011, 2014); (3) photoinactivation processes (qI) due to the photodamage of PSII (e.g. Tyystjärvi, 2013); (4) cyclic electron flow around PSI (e.g. Miyake, 2010; Buchert *et al.*, 2018), chlororespiration (Bennoun, 1982) and electron flow to molecular oxygen (Mehler, 1951; Asada, 1999); as well as (5) activation of the Calvin–Benson cycle. Therefore, besides the partial models necessary for modelling the fast ChlF rise discussed in the previous section (e.g. RRP, Kok's oxygen clock, TEG, the Q-cycle at the Cyt b_6/f complex), the processes listed above are fundamental for modelling the whole ChlFI; however, qT and qI, with a few exceptions, have been usually neglected by most authors.

Laisk *et al.* (1997) were the first to model the qE process, which they used later to simulate successfully the slow PS(M)T phase of ChlFI (Laisk *et al.*, 2006). This qE model was later adapted by Zhu *et al.* (2013) for C_3 photosynthesis, but the descending M-T phase is missing in their simulated ChlFI curve. Note that these two papers were centred on the detailed description of metabolic reactions.

The transmembrane *pmf*, i.e. both ΔpH and ΔΨ, was modelled by Lebedeva *et al.* (2002), which predicts that a sufficiently large transmembrane electric potential (positive inside) would slow the rate of PQH_2 oxidation by the Cyt b_6/f (the so-called backpressure effect; see van Kooten *et al.*, 1986), and consequently the ET rate from PSII to PSI (see also comments in Stirbet *et al.*, 2014). This *pmf* model was further used by, for example, Rubin *et al.* (2009) and Belyaeva *et al.* (2016, 2019) to model the complete ChlFI curve, with a TM model that describes the electron/proton transfer reactions between membrane protein complexes: PSII, PSI, Cyt b_6/f, mobile PQ pool in the TM, PC in lumen and Fd in stroma, CEF-PSI, and reduction of $NADP^+$ via Fd-$NADP^+$-oxidoreductase (FNR) (see Fig. 1). Belyaeva *et al.* (2016) used the TM model to fit both ChlFI data and P700 redox changes (ΔA_{810}), measured in pea leaves, from 20 µs to 20 s. Belyaeva *et al.* (2019) added to their earlier TM model partial models for the light-induced activation of FNR and qE, with the goal to simulate the ChlFI and ΔA_{810} kinetics on the time scale from 40 µs to 30 s. Their results showed that the time-dependent rate constants changed substantially upon the release of ET on the (electron) acceptor side of PSI and during qE induction. Belyaeva *et al.* (2019) also discussed differences between the parameters related to FNR activation and qE induction evaluated for dark-adapted and pre-illuminated pea leaves, and also analysed the transition between CEF-PSI and LEF modes.

Because the photosynthetic organisms are exposed continuously to fluctuations in the environmental conditions, the activity of their photosynthetic apparatus is dynamic, being feedback-regulated by several processes that reduce imbalances between the rate of energy trapping by the PSs and CO_2 assimilation. These serve to optimize the photosynthetic ET to, for example, light-induced pH changes in the lumen and in the stroma (see Tikhonov, 2013; Rochaix, 2014; Strand and Kramer, 2014), or changes in the PQ pool redox state, as modulated by variations in light irradiance, ATP/ADP ratio and the ambient CO_2 level (Rochaix, 2014, 2016). Light-induced acidification of the lumen slows down PQH_2 oxidation by the Cyt b_6/f (the backpressure effect), and also decreases PSII activity by inducing excitonic energy dissipation as heat in PSII antenna through qE (Jahns and Holzwarth, 2012; Rochaix, 2014, 2016). This reduces the excess of input energy in the system, and thus oxidative damage (Nishiyama *et al.*, 2006), which occurs when singlet excited ^{1}Chl* forms triplet-state Chl (^{3}Chl) (Durrant *et al.*, 1990) that interacts with ground state oxygen, generating 'noxious' reactive oxygen species (ROS), such as singlet oxygen ($^1O_2$). Furthermore, the alkalization of stroma activates the Calvin–Benson cycle, which stimulates the consumption of NADPH and ATP (Werdan *et al.*, 1975; Noctor and Foyer, 2000). As shown earlier, state transitions re-equilibrate PSI and PSII activities through changes in their absorption CS, which are triggered by PQ pool redox state changes (for plants and algae, see reviews by Rochaix, 2014, 2016; Goldschmidt-Clermont and Bassi, 2015), and involve phosphorylation/dephosphorylation of the PSII mobile antenna by kinases and phosphatases (i.e. STN7/TAP38 in *Arabidopsis thaliana*, or Stt7/Pph1 in *Chlamydomonas reinhardtii*; Rochaix *et al.*, 2012). Furthermore, during induction of the Calvin–Benson cycle, changes in illumination, or anaerobiosis, photosynthetic electron fluxes are optimally redistributed between the linear electron transport (LET) from water to $NADP^+$, and alternative electron pathways, i.e. cyclic electron flows, pseudocyclic O_2-dependent electron flows and the malate valve (Backhausen *et al.*, 2000; Miyake, 2010; Hemschemeier and Happe, 2011).

Modelling the state transition process

Ebenhöh *et al.* (2014) were the first to model state transitions in plants and algae based on a mechanism, described by Allen *et al.* (1981); they investigated the dynamics and regulation of state transitions by simulating experimental PAM-SP curves

from *Chlamydomonas reinhardtii* cells, grown under dim light, and thus with little capacity for qE, having a low LHCSR3 content (Peers *et al.*, 2009). Here, a simplified mathematical model (based on eight coupled ODEs) was used, where the most relevant ET routes, necessary for modelling state transitions in this green alga, were used: LEF, CEF-PSI, and chlororespiration through the plastid terminal oxidase PTOX (see Fig. 1; and Bennoun, 1982; McDonald *et al.*, 2011). Individual reactions of the Calvin–Benson cycle were treated implicitly, using steady-state consumption of NADPH and ATP, and a quasi-steady state approximation for the dynamics of oxygen evolution and charge separation in PSII. For simplicity, in the partial model of state transitions, it was assumed that the PSII mobile antennas phosphorylated by the kinase Stt7 (activated by the PQ pool reduction) are relocated directly to PSI (i.e. state 1 to state 2 transition, qT_{12}); also, after the Stt7 inhibition (triggered by the PQ pool oxidation), the PSII mobile antennas are dephosphorylated by the phosphatase Pph1, and directly re-associate with PSII (i.e. state 2 to state 1 transition, qT_{21}) (see Fig. 4). Finally, the ChlF signal is defined by the ratios of rate constants related to fluorescence emission, heat dissipation and photochemistry, which include changes in the absorption CS of PSI and PSII (due to state transition). Ebenhöh *et al.* (2014) successfully simulated with their model the main features of the experimental fluorescence signal measured with a PAM instrument from dark-adapted wild-type *Chlamydomonas* cells illuminated for 10 min with low light (100 µmol photons m^{-2} s^{-1}). The saturating F_M' peaks during illumination reflect changes in the antenna CS of PSII (i.e. a partial state transition to 'state 2'), which take place in parallel with the establishment of a stationary redox poise of the PQ pool.

State transitions were also modelled by Stirbet and Govindjee (2016), with the goal to simulate the slow PS(M)T phase of the ChlFI, in order to determine the origin of the S–M rise of *Chlamydomonas reinhardtii* cells (see Kodru *et al.*, 2015; Zhou *et al.*, 2015). Here, the photosynthesis model of Ebenhöh *et al.* (2014) was adapted for the simulation of ChlF data obtained by using a Plant Efficiency Analyser (PEA; Hansatech, UK). Stirbet and Govindjee (2016) confirmed that, under anaerobic conditions, in darkness, the PQ pool reduction through chlororespiration triggers a state 1 to state 2 transition (see Fig. 9A), when the relative CS of PSII (CSII) is lower than that of PSI (see Bulté *et al.*, 1990). Next, it was shown that, during the subsequent illumination, the hypothetical sample undergoes a transition from this 'state 2' to a 'state 1', which is the origin of the slow S-M fluorescence rise (see Fig. 9B). However, if the dark-adaptation period is too short, and the transition to 'state 2' in darkness is not complete, the subsequent illumination triggers a state 1 to state 2 transition (see Fig. 9C). We note, however, that the M-T fluorescence decline observed experimentally (Kodru *et al.*, 2015; see also Fig. 6B) is missing in the simulated curves, and, thus, further research is needed to determine its origin.

Stirbet and Govindjee (2016) also examined *in silico* the influence of different factors on the amplitude of the S-M fluorescence rise under low light conditions (~100 to 300 µmol photons m^{-2} s^{-1}). For example, they found that, under conditions that trigger a qT_{21} during a dark-to-light transition (i.e. reduced PQ pool, and CSII < 0.5 at the beginning of illumination), an increase in the CEF-PSI rate leads to a lower CSII increase at the end of the state transition, and a smaller amplitude of the S-M

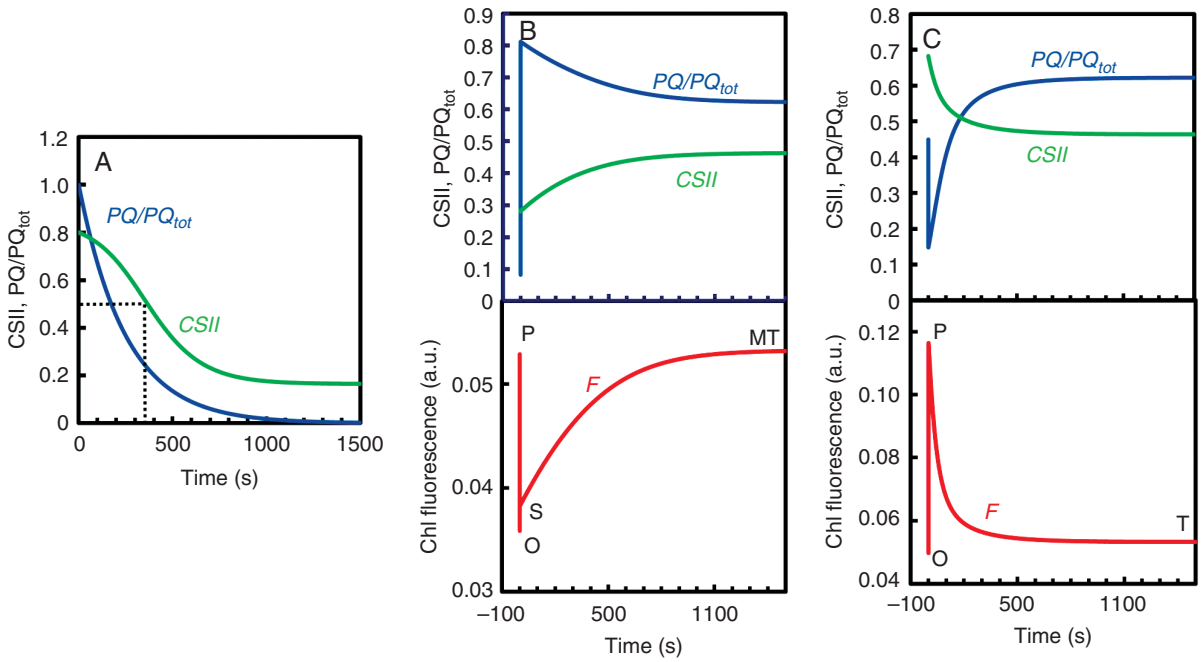

FIG. 9. Simulated kinetics of the fraction of the oxidized plastoquinone (PQ) pool (i.e. PQ/PQ_{tot}) and the relative absorption cross-section of photosystem (PS) II (i.e. CSII) during dark adaptation under anoxic conditions of a hypothetical sample of *Chlamydomonas reinhardtii* cells (see A), as well as simulated time courses of PQ/PQ_{tot}, CSII and Chl fluorescence induction (F) during illumination in the presence of oxygen of the hypothetical sample after 600 s (see B) and 200 s (see C) anoxic dark adaptation. Note that a decrease in CSII reflects a state 1 to state 2 transition, while an increase reflects a state 2 to state 1 transition. Modified from Stirbet and Govindjee (2016).

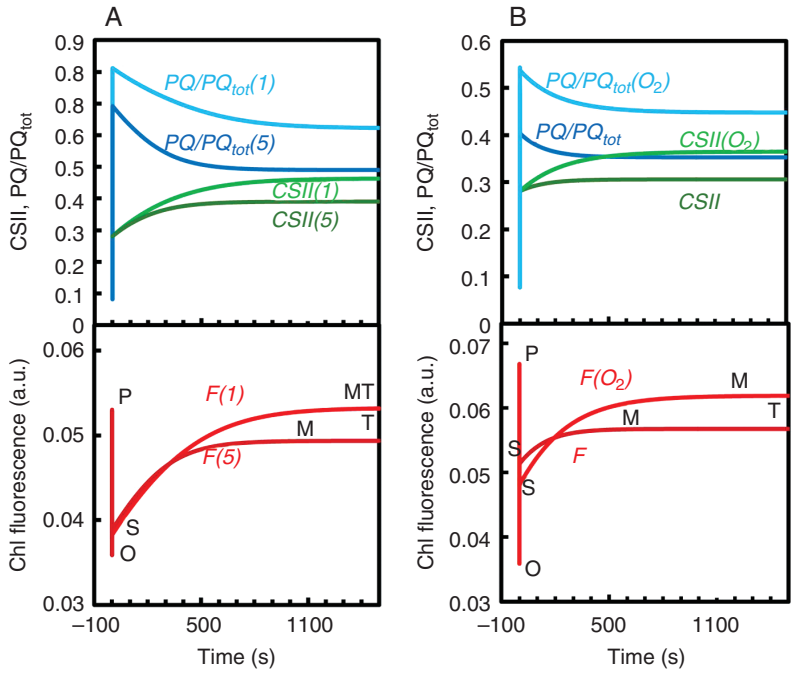

FIG. 10. Simulated kinetics of the fraction of the oxidized plastoquinone (PQ) pool (i.e. PQ/PQ_{tot}), the relative absorption cross-section of photosystem (PS) II (i.e. CSII), and of chlorophyll (Chl) fluorescence induction (F) during illumination in the presence of oxygen of a hypothetical sample of *Chlamydomonas reinharditii* cells dark-adapted for 600 s under anoxic conditions, by considering that: (1) the illumination is equivalent to 100 µmol photons m^{-2} s^{-1}, and the rate constant of the cyclic electron flow (CEF) around PSI is k_{Cyc} = 1 or 5 s^{-1} (see A); and (2) the illumination is equivalent to 300 µmol photons m^{-2} s^{-1}, the rate constant of CEF-PSI is 1 s^{-1}, and that of the Mehler reaction (i.e. ET from ferredoxin to O_2) k_{O2} = 0 or 11 s^{-1} (see B). Note that an increase in CSII reflects a state 2 to state 1 transition. These simulations show that the S-M fluorescence rise decreases when light intensity increases or when CEF-PSI is faster, but increases when the Mehler reaction is also functioning. Modified from Stirbet and Govindjee (2016).

fluorescence rise (see Fig. 10A). This simulation also confirmed that, when the CEF-PSI is much more rapid, the ATP level increases, while the NADPH level decreases. When the light intensity is higher, the simulations also showed a decrease in the S-M fluorescence rise. This result is in agreement with the experimental ChlFI data on *Chlorella* published by Papageorgiou and Govindjee (1968*a*), who showed that the slow S-M fluorescence rise is larger at lower exciting light intensities. By contrast, under other conditions taken into account by Stirbet and Govindjee (2016), such as the increase in NADPH and ATP consumption by the Calvin–Benson cycle, or an increase in the rate of the Mehler reaction, the S-M amplitude increased, due to a larger increase in the PSII CS during the qT_{21} (see Fig. 10B). However, the increase in the S-M rise becomes saturated by further increasing these rate constants. The conclusion is that the factors reducing the PQ pool (e.g. higher light intensity, or more rapid CEF-PSI) decrease the S-M amplitude, and those that oxidize further the PQ pool (e.g. more rapid NADPH consumption or Mehler reaction) increase the S-M amplitude.

Modelling the qE component of NPQ

Because NPQ in plants and algae is associated with LHCs of PSII (see Horton *et al.*, 1996; Tian *et al.*, 2017), models simulating qE usually include reactions around PSII, and focus on describing the ChlFI (see reviews by Zaks *et al.*, 2013; Matuszyńska and Ebenhöh, 2015). Different photosynthesis models have been used to simulate either ChlFI curves measured with instruments using direct light (e.g. PEA), or with PAM-SP fluorometers (for a review see Stirbet *et al.*, (2014). But, of course, the main phenomenon under analysis with either of these instruments is the same. Besides measurements of ChlF lifetime (e.g. Gilmore *et al.*, 1995, 1998; Sylak-Glassman *et al.*, 2016), measurements of Chl fluorescence yield with PAM-SP fluorometers are especially suitable for the study of NPQ processes (Müller *et al.*, 2001). It is clear that models that simulate experimental PAM data are valuable tools to analyse the qE component of NPQ.

Several original qE models have been proposed by, for example, Ebenhöh *et al.* (2011) and Zaks *et al.* (2012); these have been used for the simulation of the dynamics of ChlF quenching, as measured by PAM-SP instruments (see review by Stirbet *et al.*, 2014). Now, photosynthesis models that include qE are available (Ebenhöh *et al.*, 2014; Matuszyńska *et al.*, 2016, 2019; Snellenburg *et al.*, 2017; Morales *et al.*, 2018*a*, *b*).

The qE model of Ebenhöh *et al.* (2014) takes into account the induction of qE by low pH in the lumen (see above), but it is based on the simplifying assumption that the xanthophyll cycle is the *only* component involved in qE-dependent quenching. Thus, it was assumed that the decrease in lumenal pH leads directly to the formation of 'Z' through the xanthophyll cycle (i.e. the de-epoxidation of V via A), which then acts as a fluorescence quencher in the PSII antenna; the quencher

acts by increasing the rate constant of the non-radiative deactivation of the ^{1}Chl*. Furthermore, the qE is reversed in darkness as Z is epoxidized to V by an active epoxidase. The results of the simulations, obtained with this qE model, showed that high light illumination leads to a plateau of the PQ pool redox state, which is relatively constant for a range of CSII values. Based on these theoretical results, Ebenhöh *et al.* (2014) concluded that, due to qE induction, the requirement to adjust the antenna CS through state transition under high light is much lower than under low light conditions. Indeed. Allorent *et al.* (2013) showed that the phosphorylation of LHCII antenna, mainly mediated by the STN7/Stt7 kinase in low light, is inhibited by high light, due either to a negative regulation of the kinase through the thioredoxin pathway under high light (see e.g. Lemeille and Rochaix, 2010), or to a conformational change in the PSII antenna (Vink *et al.*, 2004).

To avoid the harmful effects of over-excitation, plants optimize their photosynthetic performance based on their illumination history through a process in which Z seems to play a key role (e.g. Ruban *et al.*, 2012). Matuszyńska *et al.* (2016) used a combined experimental and theoretical approach in the study of qE, particularly designed to determine if plants have a 'memory' of their recent (minutes to hours) light exposure, similar to what occurs after really long (days, months) periods of stress (Demmig *et al.*, 1987; Adams and Demmig-Adams, 2004). In these studies, fluorescence measurements were made on *Epipremnum aureum* (a shadow (shade)-tolerant, ornamental plant) by PAM-SP. Here, F_M' was used instead of NPQ, as suggested by Holzwarth *et al.* (2013), to avoid mathematical distortion of the ChlF quenching kinetics. Additionally, the pigment composition was measured at the end of each phase of the experiment, in order to determine the contribution of Z to the 'memory' effect. These data confirmed the presence of a short-term 'memory' effect, which is influenced by both light intensity and the period of dark-relaxation between two light exposures. Matuszyńska *et al.* (2016) concluded that the 'memory' of recent light exposure related to qE can be assigned to dynamic changes in pigment composition, being due to a slower conversion of Z to V, as observed by, for example, Demmig *et al.* (1987) and Reinhold *et al.* (2008). By implementing a qE model based on the '4 state-2-site quenching' system (Holzwarth and Jahns, 2014) in the photosynthesis model of Ebenhöh *et al.* (2014) (but without state transitions), Matuszyńska *et al.* (2016) were able to simulate successfully changes in the quantum yield of ChlF during the PAM-SP experiments, discussed above. In these simulations, the ChlF signal was also calculated using ratios of rate constants related to fluorescence emission, heat dissipation and photochemistry, where the rate constant of the heat dissipation was assumed to be modulated by the concentration of a quencher (Q), which was, in turn, calculated by taking into account the concentrations at any time of both Z and the protonated PsbS protein. [Note that Snellenburg *et al.* (2017) and Morales *et al.* (2018*a*, *b*) have used similar qE models, depending on the relative concentrations of Z and protonated PsbS.]

Modelling alternative electron flows

Besides LEF, which provides the Calvin–Benson cycle with NADPH and ATP, other ET routes function during oxygenic photosynthesis (see Fig. 1; Alric and Johnson, 2017; Shikanai and Yamamoto, 2017): (1) CEF-PSI via ferredoxin-plastoquinone reductase, or NADPH dehydrogenase (NDH); and (2) 'alternative' non-cyclic pathways that involve reduction of electron acceptors such as O_2 [the water–water cycle (WWC); see a model by Valero *et al.* (2009)], or oxaloacetate [by malate dehydrogenase (MDH); see a model by Fridlyand *et al.* (1998)]. The main role of CEF-PSI is to increase the ATP/NADPH ratio, as 'required' by the metabolic reactions in stroma or other energy-dependent processes in the chloroplast; furthermore, the pH difference, which induces qE, protects PSI and PSII against photoinhibition (Strand *et al*, 2016, 2017). The electron pathway to molecular oxygen (Mehler reaction, WWC), besides contributing to the acidification of the lumen and to the reduction of the excitation pressure on PSs, is also important in chloroplast redox signalling during abiotic stress, and in the regulation of CEF-PSI (Miyake, 2010). The respective contributions of alternative electron pathways to the total ET is strictly regulated, depending on environmental conditions, but further research is needed to understand how these diverse pathways and their regulatory mechanisms function (see Yamori *et al.*, 2016; Nawrocki *et al.*, 2019).

Comprehensive dynamic C_3 photosynthesis models, such as those by Laisk *et al.* (2006, 2009) and Zhu *et al.* (2013), include light reactions, proton and electron transport, detailed carbon metabolism reactions, exchange of intermediates between cytosol and stroma, photorespiration, amino acid synthesis, and regulatory mechanisms. However, because these models involve a large number of model parameters, simplified photosynthesis models are much more suitable, and practical, for the study of dynamic responses of the photosynthetic apparatus to diverse changes of environmental factors. Indeed, a number of simplified photosynthesis models have been used in several studies to analyse PETC regulation *in silico*, through simulation of experimental data measured with a variety of methods (Ebenhöh *et al.*, 2011; Zaks *et al.*, 2013; Tikhonov and Vershubskii, 2014; Stirbet and Govindjee, 2016; Snellenburg *et al.*, 2017; Morales *et al.*, 2018*a*, *b*; Matuszyńska *et al.*, 2016, 2019). According to Morales *et al.* (2018*b*), the term 'regulation' means: reaching simultaneously, during environmental fluctuations, a suitable redox state of PETC, dissipation of excess excitation energy and ATP/NADPH ratio through adjustments of NPQ processes, CEF-PSI and reduction of alternative electron acceptors (also including the reduction of NO_2^- during NH_4^+ assimilation, NiR), as well as *pmf* optimization through changes in ATP synthase activity.

We have reviewed above results obtained in studies of photosynthesis regulation through state transitions and qE, based on simulations of ChlFI data. By contrast, Morales *et al.* (2018*b*) used, for simulations, several types of experimental data on *Arabidopsis thaliana*, such as PAM-SP ChlF data (for effective quantum yield of PSII and NPQ), ΔA_{820} (for the P700 redox state, which is related to LET and alternative ET pathways), the electrochromic shift in A_{520} (for *pmf* and its components), and net CO_2 assimilation (A_n, for the Calvin–Benson cycle and CO_2 diffusion). The results of these simulations have shown that CEF-PSI and alternative ET pathways are strongly interacting, and, thus, changes in FQR- or NDH-dependent CEF-PSI kinetics indirectly influence WWC, NiR and MDH activities, due to changes in the redox state of Fd. It is also known that the

steady-state pH in the lumen cannot be controlled only by CEF-PSI and alternative ET, because it is also greatly affected by the pH sensitivity of qE, Cyt b_6/f and ATP synthase. Additionally, Morales *et al.* (2018*b*) have examined the influence of the ADP/ATP ratio in stroma on the metabolic regulation of ATP synthesis, and their simulations showed that there is a coordination between the regulation of Rubisco, NPQ and PETC over a large range of light intensities and CO_2 concentrations. These are important observations for programming plants for better productivity.

MODELLING THE REGULATORY DEPENDENCE BETWEEN THE LIGHT REACTIONS AND THE CARBON REACTIONS

The slow part of the ChlFI induction also reflects changes due to the induction of the Calvin–Benson cycle during a dark to light transition. The activation and gradual increase in CO_2 assimilation during this phase leads to a parallel activation of ATP synthesis and an increase in the rate of LEF, which decreases the initial excitation pressure. As a result: (1) the level of Q_A reduction decreases and photochemical quenching increases; and (2) qE decreases, because, due to a faster synthesis of ATP, the ΔpH decreases. Therefore, only models that include the induction of the Calvin–Benson cycle are suitable for correctly modelling the slow part of the ChlFI induction (see Laisk *et al.*, 2006, 2009; Zhu *et al.*, 2013).

The Calvin–Benson cycle is one of the best-studied plant metabolic processes. Besides photosynthesis models, which include both the light and carbon reactions (e.g. Laisk *et al.*, 2006, 2009; Zhu *et al.*, 2013; Belassio, 2019; Matuszyńska *et al.*, 2019), the carbon assimilation was often modelled separately, by considering a simplified relationship for NADPH and ATP supply (see review by Jablonsky *et al.*, 2011). In these models, carbon metabolism was analysed either by taking into account the kinetic properties of the enzymes involved, i.e. dynamic modelling (Pettersson and Ryde-Pettersson, 1988; Zhu *et al.*, 2007), or without the need to use these, i.e. stoichiometric modelling (Boyle and Morgan, 2009). In addition, a combination of both the above approaches has also been used (Fleming *et al.*, 2010). In many models for the Calvin–Benson cycle, the steady-state behaviour of the photosynthetic apparatus has been analysed based on the equations of Farquhar *et al.* (1980). Here we briefly mention some recent results on (short-term) regulation of photosynthesis obtained with the photosynthesis models of Morales *et al.* (2018*a*), Belassio (2019) and Matuszyńska *et al.* (2019).

Fluctuating irradiances, which were shown to limit the performance of photosynthesis (Pearcy, 1990), can be due to transient sun exposure, penumbra effects, shading by clouds, gaps in the canopy that produce ‘light (sun) flecks’, or movements of the leaves in the wind. Morales *et al.* (2018*a*) used a simplified dynamic model of CO_2 assimilation in a leaf to analyse the effects of fluctuating irradiances. In this study, they extended the canonical steady-state model by adding original empirical (phenomenological) partial models for the effects of chloroplast movement (qM; Dall’Osto *et al.*, 2014; Baránková *et al.*, 2016; Semer *et al.*, 2018, 2019), qE, qI, regulation of enzyme activity in the Calvin–Benson cycle, metabolite concentrations, and the dynamic CO_2 diffusion through different leaf compartments. Changes in qE were assumed to follow PsbS protonation and Z generation, as was the case with the approach used by Matuszyńska *et al.* (2016). With their model, Morales *et al.* (2018*a*) analysed potential improvements in CO_2 assimilation that may result after removing the kinetic limitation of different regulatory processes. Their simulations predicted that the most limiting steps in the carbon reactions are the activation rates of the Calvin–Benson cycle enzymes and stomatal opening (up to 17 % improvement), followed by the rate of qE relaxation and chloroplast movement (up to 10 % improvement), depending on the frequency of light fluctuations. However, up to 32 % improvement in CO_2 assimilation has been predicted, when all the kinetic limitations were simultaneously removed. Belassio (2019) has presented a dynamic photosynthesis model which also includes both light and carbon reactions, coupled to a mechanistic hydro-mechanical partial model for stomatal behaviour. This model successfully simulates responses to rapid changes in light intensity (light flecks), as well as in atmospheric CO_2 and O_2 concentrations. This model is freely available (as a supplement to the paper), and runs as a stand-alone workbook in Microsoft Excel.

Finally, Matuszyńska *et al.* (2019) have proposed a dynamic photosynthetic model describing the light reactions and the Calvin–Benson cycle in C_3 plants, for which they have used their earlier models [for light reactions: Ebenhöh *et al.* (2014) and Matuszyńska *et al.* (2016); for carbon reactions: Pettersson and Ryde-Pettersson (1988) and Poolman *et al.* (2000)]. This newly merged model is based on nine coupled ODEs for the PETC, and 15 coupled ODEs for the carbon reactions. Analysis of this model shows the need for a ‘stand-by’ mode of the Calvin–Benson cycle in darkness, so that it can be restarted after prolonged dark periods; in this sense, the oxidative pentose phosphate pathway can play this function. Matuszyńska *et al.* (2019) have also used MCA (e.g. Visser and Heijnen, 2002) and metabolic supply–demand analysis (Hofmeyr and Cornish-Bowden, 2000) to investigate the regulatory dependence between the PETC and the Calvin–Benson cycle, and to quantify the ‘control distribution’ of supply and demand under different light conditions and CO_2 assimilation rates. Th results obtained with MCA have indicated that, when CO_2 is saturating, the demand reactions control the flux under light-saturating conditions (with seduheptulose-1,7-*bis*phosphatase maintaining the highest overall flux control; see Poolman *et al.*, 2000), while the supply reactions display higher overall flux control under light-limited conditions, with PSII and PSI activities sustaining the highest overall flux control.

CONCLUSIONS

In this review, we have shown the important role played by models in deciphering and untangling different less well-understood and complex processes of photosynthesis, emphasizing the necessity and importance of modelling in the analysis of hypotheses developed from experimental studies. One major example, used in this review, is the ChlFI, which is simultaneously influenced by various photosynthetic processes affecting different segments of the fluorescence transient. As shown here,

this process has been simulated by many modellers, who were focused either on understanding the dynamics of the redox states of different PETC components (see also reviews by Lazár, 1999; Lazár and Schansker, 2009; Stirbet *et al.*, 2014), or that of more complex, regulatory mechanisms involved in processes such as state transitions and qE, or of the relative contributions of alternative ET pathways, as well as their relationship with the CO_2 assimilation (the Calvin–Benson cycle) (see also Stirbet *et al.*, 2014). From the examples discussed in this review, it is evident that correctly simplified but complete dynamic models of photosynthesis are well suited to obtaining information about how the photosynthetic organisms cope with variable environmental conditions (see also Matuszyńska and Ebenhöh, 2015). Indeed, modelling is a very efficient method to identify important morphological and physiological parameters of a biological system and to find their optimal values. In addition, by using a larger variety of experimental data to verify such models, the simulations can lead to much more meaningful information about the organizational principles of the photosynthetic apparatus, which can also reveal original ways and means to improve the photosynthetic efficiency of plant crops (Zhu *et al.*, 2007; Rosenthal *et al.*, 2011; Kromdijk *et al.*, 2016), besides being of theoretical interest. Moreover, multi-scale plant models (also known as plant system models), which quantitatively integrate physical, biochemical and physiological processes at different organizational levels (e.g. molecular, cell, organ, plant, population, or ecosystem), are able to predict physiological and growth properties of plants beyond photosynthetic metabolism, and they represent the future challenge in plant modelling (see Zhu *et al.*, 2016; Marshall-Colón *et al.*, 2017; Chang *et al.*, 2019; Marshall-Colón and Kliebenstein, 2019).

FUNDING

D.L. was supported by European Regional Development Fund project 'Plants as a tool for sustainable global development' [No. CZ.02.1.01/0.0/0.0/16_019/0000827].

ACKNOWLEDGEMENTS

Govindjee is grateful for IT support provided by the UIUC Life Sciences Office of Information Technology (Andrew Debevec, Karl Schlipf, Thomas Uebele, Jeffrey Haas), and the staff of the Department of Plant Biology and of the Department of Biochemistry, University of Illinois at Urbana-Champaign; he encourages all readers to visit his web site (http://www.life.illinois.edu/govindjee/) to download available educational material on photosynthesis for personal use.

LITERATURE CITED

Adams WW III, Demmig-Adams B. 2004. Chlorophyll fluorescence as a tool to monitor plant response to the environment. In: George C, Papageorgiou GC, Govindjee. eds: *Chlorophyll a fluorescence: a signature of photosynthesis. Advances in photosynthesis and respiration*. Vol. **19**. Dordrecht: Springer, 583–604.

Allen JF. 2002. Plastoquinone redox control of chloroplast thylakoid protein phosphorylation and distribution of excitation energy between photosystems: discovery, background, implications. *Photosynthesis Research* **73**: 139–148.

Allen JF. 2003. State transitions – a question of balance. *Science* **299**: 1530–1532.

Allen JF, Bennett J, Steinback KE, Arntzen CJ. 1981. Chloroplast protein phosphorylation couples plastoquinone redox state to distribution of excitation-energy between photosystems. *Nature* **291**: 25–29.

Allen MB, Whatley FR, Arnon DI. 1958. Photosynthesis with isolated chloroplasts. VI. Rates of conversion of light into chemical energy in photosynthetic phosphorylation. *Biochimica et Biophysica Acta* **27**: 16–23.

Allorent G, Tokutsu R, Roach T, *et al.* 2013. A dual strategy to cope with high light in *Chlamydomonas reinhardtii*. *Plant Cell* **25**: 545–557.

Alric J. 2010. Cyclic electron flow around photosystem I in unicellular green algae, *Photosynthesis Research* **106**: 47–56.

Alric J, Johnson X. 2017. Alternative electron transport pathways in photosynthesis: a confluence of regulation. *Current Opinion in Plant Biology* **37**: 78–86.

Antal TK, Maslakov A, Yakovleva OV, Krendeleva TE, Riznichenko GY, Rubin AB. 2018. Simulation of chlorophyll fluorescence rise and decay kinetics, and P_{700}-related absorbance changes by using a rule-based kinetic Monte-Carlo method. *Photosynthesis Research* **138**: 191–206.

Arnon DI. 1984. The discovery of photosynthetic phosphorylation. *Trends in Biochemical Sciences* **9**: 258–262.

Arnon DI, Allen MB, Whatley FR. 1954*a*. Photosynthesis by isolated chloroplasts. *Nature* **174**: 394–396.

Arnon DI, Whatley FR, Allen MB. 1954*b*. Photosynthesis by isolated chloroplasts. II. Photosynthetic phosphorylation, the conversion of light energy into phosphate bond energy. *Journal of the American Chemical Society* **76**: 6324–6329.

Asada K. 1999. The water–water cycle in chloroplasts: scavenging of active oxygens and dissipation of excess photons. *Annual Review of Plant Physiology and Plant Molecular Biology* **50**: 601–639.

Avron M. 1963. A coupling factor in photophosphorylation. *Biochimica et Biophysica Acta* **77**: 699–702.

Baake E, Schlöder JP. 1992. Modelling the fast fluorescence rise of photosynthesis. *Bulletin of Mathematical Biology* **54**: 999–1021.

Backhausen JE, Kitzmann C, Horton P, Scheibe R. 2000. Electron acceptors in isolated intact spinach chloroplasts act hierarchically to prevent overreduction and competition for electrons. *Photosynthesis Research* **64**: 1–13.

Baránková B, Lazár D, Nauš J. 2016. Analysis of the effect of chloroplast arrangement on optical properties of green tobacco leaves. *Remote Sensing of Environment* **174**: 181–196.

Bassham JA. 2005. Mapping the carbon reduction cycle: a personal perspective. In: Govindjee, Beatty JT, Gest H, Allen JF, eds. *Discoveries in photosynthesis. Advances in photosynthesis and respiration*. Dordrecht: Springer, 815–832.

Bay Z, Pearlstein RM. 1963. A theory of energy transfer in the photosynthetic unit. *Proceedings of the National Academy of Sciences of the USA* **50**: 1071–1078.

Belassio C. 2019. A generalised dynamic model of leaf-level C3 photosynthesis combining light and dark reactions with stomatal behavior. *Photosynthesis Research* **141**: 99–118.

Belyaeva NE. 2004. *Generalized model of primary photosynthetic processes in chloroplasts*. PhD thesis, Lomonosov Moscow State University.

Belyaeva NE, Bulychev AA, Riznichenko GYu, Rubin AB. 2011. A model of photosystem II for the analysis of fast fluorescence rise in plant leaves. *Biophysics* **56**: 464–477.

Belyaeva NE, Bulychev AA, Riznichenko GYu, Rubin AB. 2016. Thylakoid membrane model of the Chl *a* fluorescence transient and P700 induction kinetics in plant leaves. *Photosynthesis Research* **130**: 491–515.

Belyaeva NE, Bulychev AA, Riznichenko GYu, Rubin AB. 2019. Analyzing both the fast and the slow phases of chlorophyll a fluorescence and P700 absorbance changes in dark-adapted and preilluminated pea leaves using a thylakoid membrane model. *Photosynthesis Research* **140**: 1–19.

Benson AA. 2005. Following the path of carbon in photosynthesis: a personal story. In: Govindjee, Beatty JT, Gest H, Allen JF, eds. *Discoveries in photosynthesis. Advances in photosynthesis and respiration*. Dordrecht: Springer, 793–813.

Bennoun P. 1982. Evidence for a respiratory chain in the chloroplast. *Proceedings of the National Academy of Sciences of the USA* **79**: 4352–4356.

Blackman FF. 1905. Optima and limiting factors. *Annals of Botany* **19**: 281–295.

Blankenship RE. 2014. *Molecular Mechanisms of Photosynthesis*, 2nd edn. Oxford: Wiley-Blackwell.

Bonaventura C, Myers J. 1969. Fluorescence and oxygen evolution from *Chlorella pyrenoidosa*. *Biochimica et Biophysica Acta* **189**: 366–383.

Bouges-Bocquet B. 1973. Electron transfer between two photosystems in spinach chloroplasts. *Biochimica et Biophysica Acta* **31**: 250–256.

Boyer PD. 2002. A research journey with ATP synthase. *The Journal of Biological Chemistry* **277**: 39045–39061.

Boyle NR, Morgan JA. 2009. Flux balance analysis of primary metabolism in *Chlamydomonas reinhardtii*. *BMC Systems Biology* **3**: 4.

Breton J. 1982. The 692 nm fluorescence (F695) of chloroplasts at low temperature is emitted from the primary acceptor of photosystem II. *FEBS Letters* **147**: 16–20.

Briantais J-M, Vernotte C, Picaud M, Krause GH. 1979. A quantitative study of the slow decline of chlorophyll a fluorescence in isolated chloroplasts. *Biochimica et Biophysica Acta* **548**: 128–138.

Brooks MD, Jansson S, Niyogi KK. 2014. PsbS-dependent non-photochemical quenching. In: Demmig-Adams B, Garab G, Adams WW III, Govindjee, Sharkey TD, eds. *Nonphotochemical quenching and energy dissipation in plants, algae and cyanobacteria. Advances in photosynthesis and respiration*, vol. 40. Dordrecht: Springer, 297–314.

Buchanan BB, 2016. The carbon (formerly dark) reactions of photosynthesis. *Photosynthesis Research* **128**: 215–217.

Buchanan BB, Schürmann P, Wolosiuk RA, Jacquot JP. 2002. The ferredoxin/thioredoxin system: from discovery to molecular structures and beyond. *Photosynthesis Research* **73**: 215–222.

Buchert F, Hamon M, Gäbelein P, Scholz M, Hippler M, Wollman F. 2018. The labile interactions of cyclic electron flow effector proteins. *Journal of biological chemistry* **293**: 17559–17573.

Bulté L, Gans P, Rebeillé F, Wollman FA. 1990. ATP control on state transitions in vivo in *Chlamydomonas reinhardtii*. *Biochimica et Biophysica Acta* **1020**: 72–80.

Butler WL. 1962. Effects of red and far-red light on the fluorescence yield of chlorophyll in vivo. *Biochimica et Biophysica Acta* **64**: 309–317.

Butler WL. 1980. Energy transfer between photosystem II units in a connected package model of the photochemical apparatus of photosynthesis (photochemical model). *Proceedings of the National Academy of Sciences of the USA* **77**: 4697–4701.

Butler WL, Kitajima M. 1975. Fluorescence quenching in photosystem II of chloroplasts. *Biochimica et Biophysica Acta* **376**: 116–125.

Butler WL, Strasser RJ. 1977. Tripartite model for the photochemical apparatus of green plant photosynthesis. *Proceedings of the National Academy of Sciences of the USA* **74**: 3382–3385.

Calvin M. 1989. Forty years of photosynthesis and related activities. *Photosynthesis Research* **23**: 3–16.

Calvin M, Bassham JA, Benson AA. 1950. Chemical transformations in photosynthesis. *Federation Proceedings* **9**: 524–534.

Cardona T, Sedoud A, Cox N, Rutherford AW. 2012. Charge separation in Photosystem II: a comparative and evolutionary overview. *Biochimica et Biophysica Acta* **1817**: 26–43.

Chan HCH, Gamel OE, Fleming GR, Whaley KB. 2018. Single-photon absorption by single photosynthetic light-harvesting complexes. *Journal of Physics B: Atomic, Molecular and Optical Physics* **51**: 054002.

Chang TG, Chang S, Song QF, Perveen S, Zhu XG. 2019. Systems models, phenomics and genomics: three pillars for developing high-yielding photosynthetically efficient crops. *In silico Plants* **1**: diy003.

Chernev P, Goltsev V, Zaharieva I, Strasser RJ. 2006. A highly restricted model approach quantifying structural and fuctional parameters of photosystem II probed by the chlorophyll *a* fluorescence rise. *Ecological Engineering and Environment Protection* **2**: 19–29.

Clegg RM. 2006. The history of FRET. In: Geddes CD, Lakowicz JR, eds. *Reviews in fluorescence*. New York: Springer, 1–45.

Clegg RM, Sener M, Govindjee. 2010. From Forster resonance energy transfer (FRET) to coherent resonance energy transfer (CRET) and back – A wheen o'mickles mak's a muckle. In: Alfano RR, eds. *Optical biopsy VII*, vol. 7561. Proceedings of SPIE, 7561–7572.

Cramer WA, Kallas T, eds. 2016. *Cytochrome complexes: evolution, structures, energy transduction, and signaling. Advances in photosynthesis and respiration*, Vol. 41. Dordrecht: Springer.

Cramer WA, Hasan SS, Yamashita E. 2011. The Q cycle of cytochrome bc complexes: a structure perspective. *Biochimica et Biophysica Acta* **1807**: 788–802.

Croce R, van Amerongen H. 2013. Light-harvesting in photosystem I. *Photosynthesis Research* **116**: 153–166.

Dall'Osto L, Cazzaniga S, Wada M, Bassi R. 2014. On the origin of a slowly reversible fluorescence decay component in the Arabidopsis npq4 mutant. *Philosophical Transactions of the Royal Society B: Biological Sciences* **369**, 20130221.

Dau H. 1994. Molecular mechanism and quantitative models of variable photosystem II fluorescence. *Photochemistry and Photobiology* **60**: 1–23.

Davis GA, Kanazawa A, Schöttler MA, *et al.* 2016. Limitations to photosynthesis by proton motive force-induced photosystem II photodamage. *eLife* **5**, e16921.

Debus RJ, Barry BA, Sithole I, Babcock GT, McIntosh L. 1988. Direct mutagenesis indicates that the donor to P680+ in photosystem II is tyrosine-161 of the D1 polypeptide. *Biochemistry* **27**: 9071–9074.

Demmig-Adams B. 2003. Linking the xanthophyll cycle with thermal energy dissipation. *Photosynthesis Research* **76**: 73–80.

Demmig B, Winter K, Krüger A, Czygan F-C. 1987. Photoinhibition and zeaxanthin formation in intact leaves: a possible role of the xanthophyll cycle in the dissipation of excess light energy. *Plant Physiology* **84**: 218–224

Demmig-Adams B, Winter K, Krüger A, Czygan F-C. 1989. Zeaxathin and the induction and relaxation kinetics of the dissipation of excess excitation energy in leaves in 2% O_2, 0% CO_2. *Plant Physiology* **90**: 887–893.

Demmig-Adams B, Garab G, Adams WW III, Govindjee, Sharkey TD, eds. 2014. *Nonphotochemical quenching and energy dissipation in plants, algae and cyanobacteria. Advances in photosynthesis and respiration*, vol. 40. Dordrecht: Springer.

Dismukes GC, Siderer Y. 1980. EPR spectroscopic observations of a manganese center associated with water oxidation in spinach chloroplasts. *FEBS Letters* **121**: 78–80.

Döring G, Renger G, Vater J. Witt HT. 1969. Properties of the photoactive chlorophyll-aII in photosynthesis. *Zeitschrift für Naturforschung* **24**: 1139–1143.

Durrant J, Giorgi L, Barber J, Klug D, Porter G. 1990. Characterisation of triplet states in isolated photosystem II reaction centres: oxygen quenching as a mechanism for photodamage. *Biochimica et Biophysica Acta* **1017**: 167–175.

Duysens LNM. 1952. *Transfer of excitation energy in photosynthesis*. PhD Thesis, Leiden University.

Duysens LMN, Amesz J, Kamp BM. 1961. Two photochemical systems in photosynthesis. *Nature* **190**: 510–511.

Duysens LMN, Sweers HT. 1963. Mechanism of the two photochemical reactions in algae as studied by means of fluorescence. In: Japanese Society of Plant Physiologists, ed. *Studies on microalgae and photosynthetic bacteria*. Tokyo: University of Tokyo Press, 353–372.

Eaton-Rye JJ, Tripathy BC, Sharkey TD, eds. 2012. *Photosynthesis: plastid biology, energy conversion and carbon assimilation*. Dordrecht: Springer.

Ebenhöh O, Houwaart T, Lokstein H, Schlede S, Tirok K. 2011. A minimal mathematical model of nonphotochemical quenching of chlorophyll fluorescence. *Biosystems* **103**: 196–204.

Ebenhöh O, Fucile G, Finazzi GG, Rochaix J-D, Goldschmidt-Clermont M. 2014. Short-term acclimation of the photosynthetic electron transfer chain to changing light: a mathematical model. *Philosophical Transactions of the Royal Society B: Biological Sciences* **369**: 20130223.

Edwards GE, Black CC Jr. 1971. Isolation of mesophyll cells and bundle sheath cells from *Digitaria sanguinalis* (L.) Scop. leaves and a scanning microscopy study of the internal leaf cell morphology. *Plant Physiology* **47**: 149–156.

Emerson R. 1958. The quantum yield of photosynthesis. *Annual Review of Plant Physiology* **9**: 124.

Emerson R, Arnold W. 1932*a*. A separation of the reactions in photosynthesis by means of intermittent light. *Journal of General Physiology* **15**: 391–420.

Emerson R, Arnold W. 1932*b*. The photochemical reaction in photosynthesis. *The Journal of General Physiology* **16**: 191–205.

Emerson R, Lewis CM. 1943. The dependence of the quantum yield of *Chlorella* photosynthesis on wavelength of light. *American Journal of Botany* **30**: 165–178.

Emerson R, Chalmers RV, Cederstrand CN. 1957. Some factors influencing the long wave limit of photosynthesis. *Proceedings of the National Academy of Sciences of the USA* **43**: 133–143.

Engel GS, Calhoun TR, Read EL. *et al.* 2007. Evidence for wavelike energy transfer through quantum coherence in photosynthetic systems. *Nature* **446**: 782–786

Farquhar GD, von Caemmerer S, Berry JA. 1980. A biochemical model of photosynthetic CO_2 assimilation in leaves of C3 species. *Planta* **149**: 78–90.

Fassioli F, Dinshaw R, Arpin PC, Scholes GD. 2014. Photosynthetic light harvesting: excitons and coherence. *Journal of the Royal Society Interface* **11**: 20130901.

Feng S, Fu L, Xia Q, Tan J, Jiang Y, Guo Y. 2018. Modelling and simulation of photosystem II chlorophyll fluorescence transition from dark-adapted state to light-adapted state. *IET Systems Biology* **12**: 289–293.

Fleming RMT, Thiele I, Provan G, Nasheuer HP. 2010. Integrated stoichiometric, thermodynamic and kinetic modelling of steady state metabolism. *Journal of Theoretical Biology* **264**: 683–692.

Förster T. 1946. Energiewanderung und fluoreszenz. *Naturwissenschaften* **6**: 166–175.

Förster T. 1948. Zwischenmolekulare energiewanderung und fluoreszenz. *Annalen der Physik* **2**: 55–75.

Fridlyand LE, Backhausen JE, Scheibe R. 1998. Flux control of the malate valve in leaf cells. *Archives of Biochemistry and Biophysics* **349**: 290–298.

Gaffron H, Wohl K. 1936. Zür theorie der assimilation. *Naturwissenschaften* **24**: 103–107.

Gilmore AM. 1997. Mechanistic aspects of xanthophyll cycle dependent energy dissipation in higher plant chloroplasts and leaves. *Physiologia Plantarum* **99**: 197–209.

Gilmore AM, Hazlett TL, Govindjee. **1995.** Xanthophyll cycle dependent quenching of Photosystem II chlorophyll a fluorescence: formation of a quenching complex with a short fluorescence lifetime. *Proceedings of the National Academy of Sciences of the USA* **92**: 2273–2277.

Gilmore AM, Shinkarev VP, Hazlett TL, Govindjee. **1998.** Quantitative analysis of the effects of intra-thylakoid pH and xanthophylls cycle pigments on chlorophyll a lifetime distributions and intensity in thylakoids. *Biochemistry* **37**: 13582–13593.

Golbeck JH, ed. 2006. *Photosystem I. The light-driven plastocyanin:ferredoxin oxidoreductase. Advances in photosynthesis and respiration*, Vol. 24. Dordrecht: Springer.

Goldschmidt-Clermont M, Bassi R. 2015. Sharing light between two photosystems: mechanism of state transitions. *Current Opinion in Plant Biology* **25**: 71–78.

Goltsev V, Yordanov I. 1997. Mathematical model of prompt and delayed chlorophyll fluorescence induction kinetics. *Photosynthetica* **33**: 571–586.

Govindjee. **1995.** Sixty-three years since Kautsky: chlorophyll a fluorescence. *Australian Journal of Plant Physiology* **22**: 131–160.

Govindjee. **2004.** Chlorophyll a fluorescence: a bit of basics and history. In: Papageorgiou GC, Govindjee, eds. *Chlorophyll a fluorescence: a signature of photosynthesis*. *Advances in photosynthesis and respiration*, Vol 19. Dordrecht: Springer, 1–41.

Govindjee, Krogmann DW. 2004. Discoveries in oxygenic photosynthesis (1727–2003): a perspective: dedicated to the memories of Martin Kamen (1920–2002) and William A. Arnold (1904–2001). *Photosynthesis Research* **80**: 15–57.

Govindjee, Papageorgiou GC. 1971. Chlorophyll fluorescence and photosynthesis: fluorescence transients. In: Giese AC, ed. *Photophysiology*. New York: Academic Press, 1–46.

Govindjee, Rabinowitch EI. 1960. Two forms of chlorophyll *a* in vivo with distinct photochemical function. *Science* **132**: 355–356.

Govindjee, Renger G. 1993. In appreciation of Bessel Kok. *Photosynthesis Research* **38**: 211–213.

Govindjee, Satoh K. 1986. Fluorescence properties of chlorophyll b- and chlorophyll c-containing algae. In: Govindjee, Amesz J, Fork DC. eds. *Light emission by plants and bacteria*. Orlando: Academic Press, 497–537.

Govindjee, van Rensen JJS. 1978. Bicarbonate effects on the electron flow in isolated broken chloroplasts. *Biochimica et Biophysica Acta* **505**: 183–213.

Govindjee, Ichimura S, Cederstrand C, Rabinowitch EI. 1960. Effect of combining far-red light with shorter wave light on the excitation of fluorescence in *Chlorella*. *Archives of Biochemistry and Biophysics* **89**: 322–323.

Govindjee, Barber J, Cramer WA, et al., eds. 1986. Excitation and electron transfer in photosynthesis – special issue dedicated to Warren L Butler. *Photosynthesis Research* **10**: 147–518.

Govindjee, Beatty JT, Gest H, Allen JF, eds. 2005. *Discoveries in photosynthesis. Advances in photosynthesis and respiration*. Dordrecht: Springer.

Govindjee, Kern JF, Messinger J, Whitmarsh J. 2010. Photosystem II. In: *Encyclopedia of Life Sciences (ELS)*. Chichester: John Wiley & Sons, Ltd, 1–15.

Govindjee, Shevela D, Björn L. 2017. Evolution of the Z-scheme of photosynthesis: a perspective. *Photosynthesis Research* **133**: 5–15.

Guissé B, Srivastava A, Strasser RJ. 1995. The polyphasic rise of the chlorophyll *a* fluorescence (O-K-J-I-P) in heat stressed leaves. *Archives des Sciences - Université de Genève* **48**: 147–160.

Guo Y, Tan J. 2011. Modeling and simulation of the initial phases of chlorophyll fluorescence from photosystem II. *BioSystems* **103**: 152–157.

Guo Y, Tan J. 2014. Kinetic Monte Carlo simulation of the initial phases of chlorophyll fluorescence from photosystem II. *BioSystems* **115**: 1–4.

Hager A, Holocher K. 1994. Localization of the xanthophyll-cycle enzyme violaxanthin de-epoxidase within the thylakoid lumen and abolition of its mobility by a (light-dependent) pH decrease. *Planta* **192**: 581–589.

Harbinson J, Woodward FI. 1987. The use of light-induced absorbance changes at 820 nm to monitor the oxidation state of P-700 in leaves. *Plant, Cell & Environment* **10**: 131–140.

Heber U. 2002. Irrungen, Wirrungen? The Mehler reaction in relation to cyclic electron transport in C3 plants. *Photosynthesis Research* **73**: 223–231.

Hemschemeier A, Happe T. 2011. Alternative photosynthetic electron transport pathways during anaerobiosis in the green alga *Chlamydomonas reinhardtii*. *Biochimica et Biophysica Acta* **1807**: 919–926.

Hill R. 1937. Oxygen evolution by isolated chloroplasts. *Nature* **139**: 881–882.

Hill R, Bendall F. 1960. Function of the two cytochrome components in chloroplasts: a working hypothesis. *Nature* **186**: 136–140.

Hind G, Jagendorf AT. 1963. Separation of light and dark stages in photophosphorylation. *Proceedings of the National Academy of Sciences of the USA* **49**: 715–722.

Hofmeyr JHS, Cornish-Bowden A. 2000. Regulating the cellular economy of supply and demand. *FEBS Letters* **476**: 47–51.

Holzapfel C. 1978. Analysis of the prompt fluorescence induction by means of computer simulation of the primary photosynthetic reactions. *Zeitschrift für Naturforschung* **33c**: 402–407.

Holzapfel C, Bauer R. 1975. Computer simulation of primary photosynthetic reactions – Compared with experimental results on O_2-exchange and chlorophyll fluorescence of green plants. *Zeitschrift für Naturforschung* **30c**: 489–498.

Holzwarth A, Jahns P. 2014. Non-photochemical quenching mechanisms in intact organisms as derived from ultrafast-fluorescence kinetic studies. In: Demmig-Adams B, Garab G, Adams WW III, Govindjee, Sharkey TD, eds. *Nonphotochemical quenching and energy dissipation in plants, algae and cyanobacteria. Advances in photosynthesis and respiration*, vol. 40. Dordrecht: Springer, 129–156.

Holzwarth AR, Miloslavina Y, Nilkens M, Jahns P. 2009. Identification of two quenching sites active in the regulation of photosynthetic light-harvesting studied by time-resolved fluorescence. *Chemical Physics Letters* **483**: 262–267.

Holzwarth AR, Lenk D, Jahns P. 2013. On the analysis of non-photochemical chlorophyll fluorescence quenching curves: I. Theoretical considerations. *Biochimica et Biophysica Acta* **1827**: 786–792.

Horton P, Ruban A, Rees D, Pascal A, Noctor G, Young A. 1991. Control of the light-harvesting function of chloroplast membranes by aggregation of the LHCII chlorophyll protein complex. *FEBS Letters* **292**: 1–4.

Horton P, Ruban V, Walters RG. 1996. Regulation of light harvesting in green plants. *Annual Review of Plant Physiology and Plant Molecular Biology* **47**: 655–684.

Horton P, Johnson MP, Perez-Bueno ML, Kiss AZ, Ruban AV. 2008. Photosynthetic acclimation: does the dynamic structure and macro-organisation of photosystem II in higher plant grana membranes regulate light harvesting states? *The FEBS Journal* **275**: 1069–1079.

Hsu B-D. 1992*a*. A theoretical study on the fluorescence induction curve of spinach thylakoids in the absence of DCMU. *Biochimica et Biophysica Acta* **1140**: 30–36.

Hsu B-D. 1992*b*. The active photosystem II centers can make a significant contibution to the initial fluorescence rise from F_0 to F_i. *Plant Science* **81**: 169–174.

Hsu B-D, Lee Y-S, Jang Y-R. 1989. A method for analysis of fluorescence induction curve from DCMU-poisoned chloroplasts. *Biochimica et Biophysica Acta* **975**: 44–49.

Ishizaki A, Fleming GR. 2009. United treatment of quantum coherent and incoherent hopping dynamics in electronic energy transfer: reduced hierarchy equation approach. *The Journal of Chemical Physics* **130**: 234111.

Iwai M, Yokono M, Inada N, Minagawa J. 2010. Live-cell imaging of photosystem II antenna dissociation during state transitions. *Proceedings of the National Academy of Sciences of the USA* **107**: 2337–2342.

Jablonsky J, Lazar D. 2008. Evidence for intermediate S-states as initial phase in the process of oxygen-evolving complex oxidation. *Biophysical Journal* **94**: 2725–2736.

Jablonsky J, Bauwe H, Wolkenhauer O. 2011. Modeling the Calvin–Benson cycle. *BMC Systems Biology* **5**: 185.

Jagendorf AT. 2002. Photophosphorylation and the chemiosmotic perspective. *Photosynthesis Research* **73**: 233–241.

Jagendorf AT, Uribe E. 1966. ATP formation caused by acid-base transition of spinach chloroplasts. *Proceedings of the National Academy of Sciences of the USA* **55**: 170–177.

Jahns P, Holzwarth AR. 2012. The role of the xanthophyll cycle and of lutein in photoprotection of photosystem II. *Biochimica et Biophysica Acta* **1817**: 182–193.

Johnson MP, Ruban AV. 2011. Restoration of rapidly reversible photoprotective energy dissipation in the absence of PsbS protein by enhanced ΔpH. *Journal of Biological Chemistry* **286**: 19973–19981.

Johnson MP, Davison P, Ruban A, Horton P. 2008. The xanthophyll cycle pool size controls the kinetics of non-photochemical quenching in *Arabidopsis thaliana*. *FEBS Letters* **582**: 259–263.

Johnson MP, Zia A, Ruban AV. 2012. Elevated ΔpH restores rapidly reversible photoprotective energy dissipation in Arabidopsis chloroplasts deficient in lutein and xanthophyll cycle activity. *Planta* **235**: 193–204.

Joliot A, Joliot P. 1964. Étude cinétique de la réaction photochimique libérant l'oxygène au cours de la photosynthèse. *Comptes Rendus de l'Académie des Sciences (Paris)* **258**: 4622–4625.

Joliot P. 1965. Cinétiques de réactions liées à l'émission d'oxygène photosynthétique. *Biochimica et Biophysica Acta* **102**: 116–134.

Joliot P. 2003. Period-four oscillations of the flash-induced oxygen formation in photosynthesis. *Photosynthesis Research* **76**: 65–72.

Joliot P, Joliot A. 2003. Excitation transfer between photosynthetic units: the 1964 experiment. *Photosynthesis Research* **76**: 241–245.

Joliot P, Barbieri G, Chabaud R. 1969. Un nouveau modèle des centres photochimiques du système II. *Photochemistry and Photobiology* **10**: 309–329.

Jordan P, Fromme P, Witt HT, Klukas O, Saenger W, Krauss N. 2001. Three dimensional structure of cyanobacterial photosystem I at 2.5 Å resolution. *Nature* **411**: 909–917.

Junge W. 2004. Protons, proteins and ATP. *Photosynthesis Research* **80**: 197–221.

Kaiser E, Morales A, Harbinson J, Kromdijk J, Heuvelink E, Marcelis LFM. 2015. Dynamic photosynthesis in different environmental conditions. *Journal of Experimental Botany* **66**: 2415–2426.

Kaiser E, Kromdijk J, Harbinson J, Heuvelink E, Marcelis LFM. 2017. Photosynthetic induction and its diffusional, carboxylation and electron transport processes as affected by CO_2 partial pressure, temperature, air humidity and blue irradiance. *Annals of Botany* **119**: 191–205.

Kamen MD. 1947. *Radioactive tracers in biology*. New York: Academic Press.

Kamiya N, Shen R-J. 2003. Crystal structure of oxygen-evolving photosystem II from *Thermosynechococcus vulcanus* at 3.7-Å resolution. *Proceedings of the National Academy of Sciences of the USA* **100**: 98–103.

Kaňa R, Govindjee. **2016.** Role of ions in the regulation of light harvesting. *Frontiers in Plant Science* **7**: 1849.

Kautsky H, Hirsch A. 1931. Neue versuche zur kohlensaureassimilation. *Naturwissenschaften* **19**: 964.

Kitajima M, Butler WL. 1975. Quenching of chlorophyll fluorescence and primary photochemistry in chloroplasts by dibromothymoquinone. *Biochimica et Biophysica Acta* **723**: 105–115.

Klimov VV, Klevanik AV, Shuvalov VA, Krasnovsky AA. 1977. Reduction of pheophytin in primary light reaction of photosystem II. *FEBS Letters* **82**: 183–186.

Klimov VV, Dolan E, Ke B. 1980. EPR properties of an intermediary electron acceptor (pheophytin) in photosystem II reaction centers at cryogenic temperatures. *FEBS Letters* **112**: 97–100.

Klughammer C, Schreiber U. 1994. An improved method, using saturating light pulses, for the determination of photosystem I quantum yield via P700+-absorbance changes at 830 nm. *Planta* **192**: 261–268.

Kodru S, Malavath T, Devadasu E, *et al.* 2015. The slow S to M rise of chlorophyll *a* fluorescence induction reflects transition from state 2 to state 1 in the green alga *Chlamydomonas reinhardtii*. *Photosynthesis Research* **125**: 219–231.

Kok B. 1956. On the reversible absorption change at 705 μm in photosynthetic organisms. *Biochimica et Biophysica Acta* **22**: 399–401.

Kok B, Forbush B, McGloin M. 1970. Cooperation of charges in photosynthetic O_2 evolution. 1. A linear four step mechanism. *Photochemistry and Photobiology* **11**: 457–475.

Kramer DM, Sacksteder CA, Cruz JA. 1999. How acidic is the lumen? *Photosynthesis Research* **60**: 151–163.

Krause H, Weis W. 1991. Chlorophyll fluorescence and photosynthesis: the basics. *Annual Review of Plant Physiology and Plant Molecular Biology* **42**: 313–349.

Krey A, **Govindjee. 1964.** Fluorescence changes in Porphyridium exposed to green light of different Intensity: A new emission band at 693 nm and its significance to photosynthesis. *Proceedings of the National Academy of Sciences of the USA* **52**: 1568–1572.

Krieger A, Weis E. 1993. The role of calcium in the pH-dependent control of photosystem II. *Photosynthesis Research* **37**: 117–130.

Krogmann DW, Jagendorf AT, Avron M. 1959. Uncouplers of spinach chloroplast photosynthetic phosphorylation. *Plant Physiology* **34**: 272–277.

Kromdijk J, Głowacka K, Leonelli L, *et al.* 2016. Improving photosynthesis and crop productivity by accelerating recovery from photoprotection. *Science* **354**: 857–861.

Kroon BMA, Thoms S. 2006. From electron to biomass: a mechanistic model to describe phytoplankton photosynthesis and steady-state growth mates. *Journal of Phycology* **42**: 593–609.

Kuvykin IV, Vershubskii AV, Priklonskii VI, Tikhonov AN. 2009. Computer simulation study of pH-dependent regulation of electron transport in chloroplasts. *Biophysics* **54**: 455–464.

Laisk A, Oja V. 2018. Kinetics of photosystem II electron transport: a mathematical analysis based on chlorophyll fluorescence induction. *Photosynthesis Research* **136**: 63–82.

Laisk A, Oja V, Rasulov B, Eichelmann H, Sumberg A. 1997. Quantum yields and rate constants of photochemical and nonphotochemical excitation quenching. Experiment and model. *Plant Physiology* **115**: 803–815.

Laisk A, Eichelmann H, Oja V. 2006. C3 photosynthesis in silico. *Photosynthesis Research* **90**: 45–66.

Laisk A, Eichelmann H, Oja V. 2009. Leaf C_3 photosynthesis *in silico*: Integrated carbon/nitrogen metabolism. In: Laisk A, Nedbal AL, Govindjee, eds. *Photosynthesis in silico: understanding complexity from molecules to ecosystems. Advances in photosynthesis and respiration*, Vol. 29. Dordrecht: Springer, 295–322.

Latimer P, Bannister TT, Rabinowitch E. 1956. Quantum yields of fluorescence of plant pigments. *Science* **124**: 585–586.

Lavergne J, Trissl H-W. 1995. Theory of fluorescence induction in photosystem II: Derivation of analytical expressions in a model including exciton-radical-pair equilibrium and restricted energy transfer between photosynthetic units. *Biophysical Journal* **68**: 2474–2492.

Lazár D. 1999. Chlorophyll *a* fluorescence induction. *Biochimica et Biophysica Acta* **1412**: 1–28.

Lazár D. 2003. Chlorophyll *a* fluorescence rise induced by high light illumination of dark-adapted plant tissue studied by means of a model of photosystem II and considering photosystem II heterogeneity. *Journal of Theoretical Biology* **220**: 469–503.

Lazár D. 2006. The polyphasic chlorophyll *a* fluorescence rise measured under high intensity of exciting light. *Functional Plant Biology* **33**: 9–30.

Lazár D. 2009. Modelling of light-induced chlorophyll *a* fluorescence rise (O-J-I-P transient) and changes in 820 nm-transmittance signal of photosynthesis. *Photosynthetica* **47**: 483–498.

Lazár D. 2013. Simulations show that a small part of variable chlorophyll a fluorescence originates in photosystem I and contributes to overall fluorescence rise. *Journal of Theoretical Biology* **335**: 249–264.

Lazár D. 2015. Parameters of photosynthetic energy partitioning. *Journal of Plant Physiology* **175**: 131–147.

Lazár D, Jablonský J. 2009. On the approaches applied in formulation of a kinetic model of photosystem II: different approaches lead to different

simulations of the chlorophyll a fluorescence transients. *Journal of Theoretical Biology* **257**: 260–269.

Lazár D, Pospíšil P. 1999. Mathematical simulation of chlorophyll *a* fluorescence rise measured with 3-(3′,4′-dichlorophenyl)-1,1-dimethylurea-treated barley leaves at room and high temperatures. *European Biophysics Journal* **28**: 468–477.

Lazár D, Schansker G. 2009. Models of chlorophyll *a* fluorescence transients. In: Laisk A, Nedbal L, Govindjee, eds. *Photosynthesis in silico: understanding complexity from molecules to ecosystems. Advances in photosynthesis and respiration*, Vol. 29. Dordrecht: Springer, 85–123.

Lazár D, Nauš J, Matoušková M, Flašarová M. 1997. Mathematical modeling of changes in chlorophyll fluorescence induction caused by herbicides. *Pesticide Biochemistry and Physiology* **57**: 200–210.

Lazár D, Brokeš M, Nauš J, Dvořák L. 1998. Mathematical modelling of 3-(3′,4′-dichlorophenyl)-1,1-dimethylurea action in plant leaves. *Journal of Theoretical Biology* **191**: 79–86.

Lazár D, Tomek P, Ilík P, Nauš J. 2001. Determination of the antenna heterogeneity of Photosystem II by direct simultaneous fitting of several fluorescence rise curves measured with DCMU at different light intensities. *Photosynthesis Research* **68**: 247–257.

Lazár D, Ilík P, Kruk J, Strzalka K, Nauš J. 2005. A theoretical study on effect of the initial redox state of cytochrome b559 on maximal chlorophyll fluorescence level (F_M). Implications for photoinhibition of photosystem II. *Journal of Theoretical Biology* **233**: 287–300.

Lebedeva GV, Belyaeva NE, Demin OV, Riznichenko GYu, Rubin AB. 2002. Kinetic model of primary photosynthetic processes in chloroplasts. Description of the fast phase of chlorophyll fluorescence induction under different light intensities. *Biophysics (Russia)* **47**: 968–980.

Lemeille S, Rochaix JD. 2010. State transitions at the crossroad of thylakoid signalling pathways. *Photosynthesis Research* **106**: 33–46.

Li X-P, Björkman O, Shih C, *et al.* 2000. A pigment-binding protein essential for regulation of photosynthetic light harvesting. *Nature* **403**: 391–395.

Long SP, Zhu XG, Naidu SL, Ort DR. 2006. Can improvement in photosynthesis increase crop yields? *Plant, Cell and Environment* **29**: 315–330.

Long SP, Marshall-Colon A, Zhu XG. 2015. Meeting the global food demand of the future by engineering crop photosynthesis and yield potential. *Cell* **161**: 56–66.

Lubitz W, Chrysina M, Cox N. 2019. Water oxidation in photosystem II. *Photosynthesis Research* **142**: 105–125.

Lyu H, Lazár D. 2017*a*. Modeling the light-induced electric potential difference ($\Delta\Psi$), the pH difference (ΔpH) and the proton motive force across the thylakoid membrane in C3 leaves. *Journal of Theoretical Biology* **413**: 11–23.

Lyu H, Lazár D. 2017*b*. Modeling the light-induced electric potential difference $\Delta\Psi$ across the thylakoid membrane based on the transition state rate theory. *Biochimica et Biophysica Acta* **1858**: 239–248.

Magyar M, Sipka G, Kovács L, *et al.* 2018. Rate-limiting steps in the dark-to-light transition of Photosystem II - revealed by chlorophyll-*a* fluorescence induction. *Scientific Reports* **8**: 2755.

Makarov S, Grachev EA, Antal TK. 2012. Mathematical modeling of photosynthetic electron transport chain considering spatial heterogeneity of the thylakoid membrane. *Mathematical Biology and Bioinformatics* **7**: 508–528.

Malkin S. 1966. Fluorescence induction studies in isolated chloroplasts. II. Kinetic analysis of the fluorescence intensity dependence on time. *Biochimica et Biophysica Acta* **123**: 433–442.

Malkin S, Kok B. 1966. Fluorescence induction studies in isolated chloroplasts. I. Number of components involved in the reaction and quantum yields. *Biochimica et Biophysica Acta* **123**: 413–432.

Malnoë A. 2018. Photoinhibition or photoprotection of photosynthesis? Update on the (newly termed) sustained quenching component qH. *Environmental and Experimental Botany* **154**: 123–133.

Mar T, Govindjee. **1972.** Kinetic models of oxygen evolution in photosynthesis. *Journal of Theoretical Biology* **36**: 427–446.

Marshall-Colón A, Kliebenstein DJ. 2019. Plant networks as traits and hypotheses: moving beyond description. *Trends of Plant Science* **24**: 840–852.

Marshall-Colón A, Long SP, Douglas K, *et al.* 2017. Crops in silico: generating virtual crops using an integrative and multi-scale modeling platform. *Frontiers in Plant Science* **8**: 786.

Maslakov AS, Antal TK, Riznichenko GY, Rubin AB. 2016. Modeling of primary photosynthetic processes using the kinetic Monte Carlo method. *Biophysics* **61**: 387–399.

Matsuoka T, Tanaka S, Ebina K. 2015. Systems approach to excitation-energy and electron transfer reaction networks in photosystem II complex: model studies for chlorophyll a fluorescence induction kinetics. *Journal of Theoretical Biology* **380**: 220–237.

Matuszyńska A, Ebenhöh O. 2015. A reductionist approach to model photosynthetic self-regulation in eukaryotes in response to light. *Biochemical Society Transactions* **43**: 1133–1139.

Matuszyńska A, Heidari S, Jahns P, Ebenhöh O. 2016. A mathematical model of non-photochemical quenching to study short-term light memory in plants. *Biochimica et Biophysica Acta* **1857**: 1860–1869.

Matuszyńska A, Saadat NP, Ebenhöh O. 2019. Balancing energy supply during photosynthesis - a theoretical perspective. *Physiologia Plantarum* **166**: 392–402.

McAlister ED, Myers J. 1940. Time course of photosynthesis and fluorescence. *Science* **92**: 241–243.

McDonald AE, Ivanov AG, Bode R, Maxwell DP, Rodermel SR, Hüner NP. 2011. Flexibility in photosynthetic electron transport: the physiological role of plastoquinol terminal oxidase (PTOX). *Biochimica et Biophysica Acta* **1807**: 954–967.

McGrath JM, Long SP. 2016. Can the cyanobacterial carbon-concentrating mechanism increase photosynthesis in crop species? A theoretical analysis. *Plant Physiology* **164**: 2247–2261.

Mehler AH. 1951. Studies on reactions of illuminated chloroplasts. I. Mechanisms of the reduction of oxygen and other Hill reagents. *Archives of Biochemistry and Biophysics* **33**: 65–77.

Melis A, Homann PH. 1975. Kinetic analysis of the fluorescence induction in 3-(3′,4′-dichlorophenyl)-1,1-dimethylurea poisoned chloroplasts. *Photochemistry and Photobiology* **21**: 431–437.

Mirkovic T, Ostroumov, Anna JM, van Grondelle R, Govindjee, Scholes GD. 2017. Light absorption and energy transfer in the antenna complexes of photosynthetic organisms. *Chemical Reviews* **117**: 249–293.

Mishra KB, Mishra A, Kubásek J, Urban O, Heyer AG, Govindjee. **2019.** Low temperature induced modulation of photosynthetic induction in non-acclimated and cold-acclimated *Arabidopsis thaliana*: chlorophyll a fluorescence and gas-exchange measurements. *Photosynthesis Research* **139**: 123–143.

Mitchell P. 1961*a*. Coupling of phosphorylation to electron and hydrogen transfer by a chemiosmotic type of mechanism. *Nature* **191**: 144–148.

Mitchell P. 1961*b*. *Chemiosmotic coupling in oxidative and photosynthetic phosphorylation*. Bodmin: Glynn Research.

Mitchell P. 1975. Protonmotive Q-cycle-general formulation. *FEBS Letters* **59**: 137–139.

Miyake C. 2010. Alternative electron flows (water–water cycle and cyclic electron flow around PSI) in photosynthesis: molecular mechanisms and physiological functions. *Plant and Cell Physiology* **51**: 1951–1963.

Morales A, Kaiser E, Yin X, *et al.* 2018*a*. Dynamic modelling of limitations on improving leaf CO_2 assimilation under fluctuating irradiance. *Plant, Cell & Environment* **41**: 589–604.

Morales A, Yin X, Harbinson J, *et al.* 2018*b*. In silico analysis of the regulation of the photosynthetic electron transport chain in C3 plants. *Plant Physiology* **176**: 1247–1261.

Müh F, Glöckner C, Hellmich J, Zouni A. 2012. Light-induced quinone reduction in photosystem II. *Biochimica et Biophysica Acta* **1817**: 44–65.

Müller P, Li X, Niyogi KK. 2001. Non-photochemical quenching. A response to excess light energy. *Plant Physiology* **125**: 1558–1566.

Munday JC, Govindjee. **1969.** Light-induced changes in the fluorescence yield of chlorophyll *a* in vivo. III. The dip and the peak in the fluorescence transient of *Chlorella pyrenoidosa*. *Biophysical Journal* **9**: 1–21.

Murata N. 1969*a*. Control of excitation transfer in photosynthesis. I. Light-induced change of chlorophyll *a* fluorescence in *Porphyridium cruentum*. *Biochimica et Biophysica Acta* **172**: 242.

Murata N. 1969*b*. Control of excitation transfer in photosynthesis. II. Magnesium ion-dependent distribution of excitation energy between two pigment systems in spinach chloroplasts. *Biochimica et Biophysica Acta* **189**: 171–181.

Murata N, Allakhverdiev SI, Nishiyama Y. 2012. The mechanism of photoinhibition in vivo: re-evaluation of the roles of catalase, α-tocopherol, non-photochemical quenching, and electron transport. *Biochimica et Biophysica Acta* **1817**: 1127–1133.

Myers J. 1994. The 1932 experiments. *Photosynthesis Research* **40**: 303–310.

Najafpour MM, Moghaddam NA, Allakhverdiev SI, **Govindjee. 2012.** Biological water oxidation: Lessons from nature. *Biochimica et Biophysica Acta* **1817**: 1110–1121.

Nawrocki WJ, Bailleul B, Picot D, *et al.* 2019. The mechanism of cyclic electron flow. *Biochimica et Biophysica Acta* **1860**: 433–438.

Nedbal L, Samson G, Whitmarsh J. 1992. Redox state of one-electron component controls the rate of photoinhibition of photosystem II. *Proceedings of the National Academy of Sciences of the USA* **89**: 7929–7933.

Nedbal L, Červený J, Schmidt H. 2009. Scaling and integration of kinetic models of photosynthesis: towards comprehensive e-photosynthesis. In: Laisk A, Nedbal AL, Govindjee, eds. *Photosynthesis in silico: understanding complexity from molecules to ecosystems. Advances in photosynthesis and respiration*, Vol. 29. Dordrecht: Springer, 17–29.

Nelson N, Junge W. 2015. Structure and energy transfer in photosystems of oxygenic photosynthesis. *Annual Review of Biochemistry* **84**: 659–683.

Nickelsen K. 2016. *Explaining photosynthesis: models of biochemical mechanisms, 1840–1960*. Dordrecht: Springer.

Nickelsen K, Govindjee. **2011.** *The maximum quantum yield controversy: Otto Warburg and the Midwest Gang*. Bern Studies in the History and Philosophy of Science, Switzerland: Berne: University of Bern, Institute für Philosophie.

Nikkanen L, Rintamäki E. 2019. Chloroplast thioredoxin systems dynamically regulate photosynthesis in plants. *Biochemical Journal* **476**: 1159–1172.

Nishiyama Y, Allakhverdiev SI, Murata N. 2006. A new paradigm for the action of reactive oxygen species in the photoinhibition of photosystem II. *Biochimica et Biophysica Acta* **1757**: 742–749.

Nižnan J. 2014. *Compact representation of photosynthesis biochemical processes*. Diploma Thesis, Masaryk University.

Noctor G, Foyer CH. 2000. Homeostasis of adenylate status during photosynthesis in a fluctuating environment. *Journal of Experimental Botany* **51**: 347–356.

Oettmeier W, Masson K, Johanningmeier U. 1980. Photoaffinity labelling of the photosystem II herbicide binding protein. *FEBS Letters* **118**: 267–270.

Okayama S, Butler WL. 1972. The influence of cytochrome b 559 on the fluorescence yield of chloroplasts at low temperature. *Biochimica et Biophysica Acta* **267**: 523–527.

Ono T, Inoue Y. 1988. Discrete extraction of the Ca atom functional for O_2 evolution in higher plant Photosystem II by a simple low pH treatment. *FEBS Letters* **227**: 147–152.

Ort DR, Merchant SS, Alric J, *et al.* 2015. Redesigning photosynthesis to sustainably meet global food and bioenergy demand. *Proceedings of the National Academy of Sciences of the USA* **112**: 8529–8536.

Osmond B, Chow WS, Wyber R, *et al.* 2017. Relative functional and optical absorption cross-sections of PSII and other photosynthetic parameters monitored in situ, at a distance with a time resolution of a few seconds, using a prototype light induced fluorescence transient (LIFT) device. *Functional Plant Biology* **44**: 985–1006.

Page CC, Moser CC, Chen X, Dutton PL. 1999. Natural engineering principles of electron tunnelling in biological oxidation-reduction. *Nature* **402**: 47–52.

Paillotin G. 1976. Movement of excitations in the photosynthetic domains of photosystem II. *Journal of Theoretical Biology* **58**: 237–252.

Papageorgiou GC. 1975. Chlorophyll fluorescence: an intrinsic probe of photosynthesis. In: Govindjee, ed. *Bioenergetics of photosynthesis*. New York: Academic Press, 319–372.

Papageorgiou GC, Govindjee. **1968*a*.** Light-induced changes in the fluorescence yield of chlorophyll a in vivo. I. *Anacystis nidulans*. *Biophysical Journal* **8**: 1299–1315.

Papageorgiou GC, Govindjee. **1968*b*.** Light induced changes in the fluorescence yield of chlorophyll a in vivo. II. *Chlorella pyrenoidosa*. *Biophysical Journal* **8**: 1316–1328.

Papageorgiou GC, Govindjee, eds. 2004. *Chlorophyll a fluorescence: a signature of photosynthesis. Advances in photosynthesis and respiration*, Vol. 19. Dordrecht: Springer.

Papageorgiou GC, Govindjee. **2011.** Photosystem II fluorescence: slow changes–scaling from the past. *Journal of Photochemistry and Photobiology B: Biology* **104**: 258–270.

Papageorgiou GC, Govindjee. **2014.** The non-photochemical quenching of the electronically excited state of chlorophyll a in plants: definitions, timelines, viewpoints, open questions. In: Demmig-Adams B, Garab G, Adams WW III, Govindjee, Sharkey TD, eds. *Nonphotochemical quenching and energy dissipation in plants, algae and cyanobacteria. Advances in photosynthesis and respiration*, vol. 40. Dordrecht: Springer, 1–44.

Papageorgiou GC, Tsimilli-Michael M, Stamatakis K. 2007. The fast and slow kinetics of chlorophyll *a* fluorescence induction in plants, algae and cyanobacteria: a viewpoint. *Photosynthesis Research* **94**: 275–290.

Pearcy RW. 1990. Sunflecks and photosynthesis in plant canopies. *Annual Review of Plant Biology* **41**: 421–453.

Peers G, Truong TB, Ostendorf E, *et al.* 2009. An ancient light-harvesting protein is critical for the regulation of algal photosynthesis. *Nature* **462**: 518–521.

Pettersson G, Ryde-Pettersson U. 1988. A mathematical model of the Calvin photosynthesis cycle. *European Journal of Biochemistry* **175**: 661–672.

Petrouleas V, Crofts AR. 2005. The quinone iron acceptor complex. In: Wydrzynski T, Satoh K. eds. *Photosystem II: the light-driven water: plastoquinone oxidoreductase. Advances in photosynthesis and respiration*, Vol. 22. Dordrecht: Springer, 177–206.

Pfündel E. 1998. Estimating the contribution of photosystem I to total leaf chlorophyll fluorescence. *Photosynthesis Research* **56**: 185–195.

Poolman MG, Fell DA, Thomas S. 2000. Modelling photosynthesis and its control. *Journal of Experimental Botany* **51**: 319–328.

Pribil M, Sandoval-Ibáñez O, Xu W. *et al.* 2018. Fine-tuning of photosynthesis requires CURVATURE THYLAKOID1-mediated thylakoid plasticity. *Plant Physiology* **176**: 2351–2364.

Rabinowitch EI. 1945. *Photosynthesis and related processes, vol 1. Chemistry of photosynthesis, chemosynthesis and related processes in vitro and in vivo*. New York: Interscience Publishers.

Rabinowitch EI, Govindjee. **1969.** *Photosynthesis*. Chichester: Wiley & Sons.

Rees D, Young A, Noctor G, Britton G, Horton P. 1989. Enhancement of the pH-dependent dissipation of excitation energy in spinach chloroplasts by light-activation: correlation with the synthesis of zeaxanthin. *FEBS Letters* **256**: 85–90.

Rees D, Noctor G, Ruban AV, Crofts J, Young A, Horton P. 1992. pH dependent chlorophyll fluorescence quenching in spinach thylakoids from light treated or dark adapted leaves. *Photosynthesis Research* **31**: 11–19.

Reinhold C, Niczyporuk S, Beran K, Jahns P. 2008. Short-term down-regulation of zeaxanthin epoxidation in *Arabidopsis thaliana* in response to photooxidative stress conditions. *Biochimica et Biophysica Acta* **1777**: 462–469.

Renger G, Schulze A. 1985. Quantitative analysis of fluorescence induction curves in isolated spinach chloroplasts. *Photobiochemistry and Photobiophysics* **9**: 79–87.

Renger G, Govindjee, eds. 1993. How plants and cyanobacteria make oxygen: 25 years of period four oscillations. *Photosynthesis Research* **38**: 211–469.

Robinson HH, Crofts AR, **1983.** Kinetics of the changes in oxidation-reduction reactions of the photosystem II quinone acceptor complex, and the pathway for deactivation. *FEBS Letters* **153**: 221–226.

Rochaix J-D. 2014. Regulation and dynamics of the light-harvesting system. *Annual Review of Plant Biology* **65**: 287–309.

Rochaix J-D. 2016. The dynamics of the photosynthetic apparatus in algae. In: Najafpour MM, ed. *Applied photosynthesis - new progress*. London: IntechOpen, 23–52.

Rochaix JD, Lemeille S, Shapiguzov A, *et al.* 2012. Protein kinases and phosphatases involved in the acclimation of the photosynthetic apparatus to a changing light environment. *Philosophical Transactions of the Royal Society B: Biological Sciences* **367**: 3466–3474.

Roden JJJ, Bennett DIG, Whaley KB. 2016. Long-range energy transport in photosystem II. *The Journal of Chemical Physics* **144**: 245101.

Roelofs TA, Lee C-H, Holzwarth AR. 1992. Global target analysis of picosecond fluorescence kinetics from pea chloroplasts. A new approach to the characterization of the primary processes in photosystem II α- and β-units. *Biophysical Journal* **61**: 1147–1163.

Rosenthal DM, Locke AM, Khozaei M, Raines CA, Long SP, Ort DR. 2011. Over-expressing the C3 photosynthesis cycle enzyme sedoheptulose-1–7 bisphosphatase improves photosynthetic carbon gain and yield under fully open air CO_2 fumigation (FACE). *BMC Plant Biology* **11**: 123.

Ruban AV, Johnson MP, Duffy CD. 2012. The photoprotective molecular switch in the photosystem II antenna. *Biochimica et Biophysica Acta* **1817**: 167–181.

Ruben S, Kamen MD. 1941. Long-lived radioactive carbon: C14. *Physics Reviews* **59**: 349–354.

Ruben S, Hassid WZ, Kamen MD. 1939. Radioactive carbon in the study of photosynthesis. *Journal of the American Chemical Society* **61**: 661–663.

Ruben S, Randall M, Kamen M, Logan Hyde JL. 1941. Heavy oxygen (^{18}O) as a tracer in the study of photosynthesis. *Journal of the American Chemical Society* **63**: 877–879.

Rubin A, Riznichenko G. 2009. Modeling of the primary processes in a photosynthetic membrane. In: Laisk A, Nedbal AL, Govindjee, eds. *Photosynthesis in silico: understanding complexity from molecules to ecosystems. Advances in photosynthesis and respiration*, Vol. 29. Dordrecht: Springer, 151–176.

Šafránek D, Červený J, Klement M, Pospíšilová J, Brim L, Lazár D, Nedbal L. 2011. E-photosynthesis: Web-based platform for modeling of complex photosynthetic processes. *BioSystems* **103**: 115–124.

Sapozhnikov DI, Krasnovskaya TA, Maevskaya AN. 1957. Change in the interrelationship of the basic carotenoids of the plastids of green leaves under the action of light. *Doklady Akademii Nauk SSSR* **113**: 465–467.

Schansker G, Srivastava A, Govindjee, Strasser RJ. 2003. Characterization of the 820-nm transmission signal paralleling the chlorophyll *a* fluorescence rise (OJIP) in pea leaves. *Functional Plant Biology* **30**: 785–796

Schansker G, Tóth SZ, Strasser RJ. 2005. Methylviologen and dibromorhymoquinone treatments of pea leaves reveal the role of photosystem I in the Chl *a* fluorescence rise OJIP. *Biochimica et Biophysica Acta* **1706**: 250–261.

Schansker G, Tóth SZ, Kovács L, Holzwarth AR, Garab G. 2011. Evidence for a fluorescence yield change driven by a light-induced conformational change within photosystem II during the fast chlorophyll *a* fluorescence rise. *Biochimica et Biophysica Acta* **1807**: 1032–1043.

Schansker G, Tóth SZ, Holzwarth AR, Garab G. 2014. Chlorophyll *a* fluorescence: beyond the limits of the Q_A model. *Photosynthesis Research* **120**: 43–58.

Schatz GH, Brock H, Holzwarth AR. 1988. Kinetic and energetic model for the primary processes in photosystem II. *Biophysical Journal* **54**: 397–405.

Schlodder E, Meyer B. 1987. pH-dependence of oxygen evolution and reduction kinetics of photooxidized chlorophyll a II (P-680) in Photosystem II particles from *Synechococcus sp*. *Biochimica et Biophysica Acta* **890**: 23–31.

Schreiber U. 1986. Detection of rapid induction kinetics with a new type of high-frequency modulated chlorophyll fluorometer. *Photosynthesis Research* **9**: 261–272.

Schreiber U, Schliwa U, Bilger W. 1986. Continuous recording of photochemical and nonphotochemical chlorophyll fluorescence quenching with a new type of modulation fluorometer. *Photosynthesis Research* **10**: 51–62.

Schreiber U, Neubauer C, Klughammer C. 1989. Devices and methods for room-temperature fluorescence analysis. *Philosophical Transactions of the Royal Society B* **323**: 241–251.

Schreiber U, Klughammer C, Schansker G. 2019. Rapidly reversible chlorophyll fluorescence quenching induced by pulses of supersaturating light in vivo. *Photosynthesis Research* **142**: 35–50.

Semer J, Štroch M, Špunda V, Navrátil M. 2018. Partitioning of absorbed light energy within photosystem II in barley can be affected by chloroplast movement. *Journal of Photochemistry and Photobiology B: Biology* **186**: 98–106.

Semer J, Navrátil M, Špunda V, Štroch M. 2019. Chlorophyll fluorescence parameters to assess utilization of excitation energy in photosystem II independently of changes in leaf absorption. *Journal of Photochemistry and Photobiology B: Biology* **197**: 111535.

Sétif P. 2015. Electron-transfer kinetics in cyanobacterial cells: Methyl viologen is a poor inhibitor of linear electron flow. *Biochimica et Biophysica Acta* **1847**: 212–222.

Shen JR. 2015. The structure of photosystem II and the mechanism of water oxidation in photosynthesis. *Annual Review of Plant Biology* **66**: 23–48.

Shevela D, Eaton-Rye JJ, Shen JR, Govindjee. **2012.** Photosystem II and the unique role of bicarbonate: a historical perspective. *Biochimica et Biophysica Acta* **1817**: 1134–1151.

Shevela D, Björn L, Govindjee. **2019.** *Photosynthesis: solar energy for life*. Singapore: World Scientific.

Shikanai TI, Yamamoto H. 2017. Contribution of cyclic and pseudo-cyclic electron transport to the formation of proton motive force in chloroplasts. *Molecular Plant* **10**: 20–29.

Shinkarev VP, Govindjee. **1993.** Insight into the relationship of chlorophyll a fluorescence yield to the concentration of its natural quenchers in oxygenic photosynthesis. *Proceedings of the National Academy of Sciences of the USA* **90**: 7466–7469.

Simkin AJ, McAusland L, Headland LR, Lawson T, Raines CA. 2015. Multigene manipulation of photosynthetic carbon assimilation increases CO_2 fixation and biomass yield in tobacco. *Journal of Experimental Botany* **66**: 4075–4090.

Simkin AJ, McAusland L, Lawson T, Raines CA. 2017. Overexpression of the RieskeFeS protein increases electron transport rates and biomass yield. *Plant Physiology* **175**: 134–145.

Simkin AJ, López-Calcagno PE, Raines CA. 2019. Feeding the world: improving photosynthetic efficiency for sustainable crop production. *Journal of Experimental Botany* **70**: 1119–1140.

Snellenburg J, Johnson MP, Ruban AV, van Grondelle R, van Stokkum IHM. 2017. A four state parametric model for the kinetics of the non-photochemical quenching in Photosystem II. *Biochimica et Biophysica Acta* **1858**: 854–864.

South PF, Cavanagh AP, Lopez-Calcagno PE, Raines CA, Ort DR. 2018. Optimizing photorespiration for improved crop productivity. *Journal of Integrative Plant Biology* **60**: 1217–1230.

Srivastava A, Guissé B, Greppin H, Strasser RJ. 1997. Regulation of antenna structure and electron transport in photosystem II of *Pisum sativum* under elevated temperature probed by the fast polyphasic chlorophyll *a* fluorescence transient: OKJIP. *Biochimica et Biophysica Acta* **1320**: 95–106.

Steffen R, Christen G, Renger G. 2001. Time-resolved monitoring of flash-induced changes of fluorescence quantum yield and decay of delayed light emission in oxygen-evolving photosynthetic organisms. *Biochemistry* **40**:173–180.

Steffen R, Eckert H-J, Kelly AA, Dörmann P, Renger G. 2005. Investigation on the reaction pattern of photosystem II in leaves from *Arabidopsis thaliana* by time resolved fluorometric analysis. *Biochemistry* **44**: 3123–3133.

Stiehl HH, Witt HT. 1968. Die kurzzeitigen ultravioletten Differenzspektren bei der Photosynthese. *Zeitschrift für Naturforschung* **23b**: 220–224.

Stiehl HH, Witt HT. 1969. Quantitative treatment of the function of plastoquinone in photosynthesis. *Zeitschrift für Naturforschung* **24b**: 1588–1598.

Stirbet A. 2013. Excitonic connectivity between photosystem II units: what is it, and how to measure it? *Photosynthesis Research* **116**. 189–214.

Stirbet A, Govindjee. **2011.** On the relation between the Kautsky effect (chlorophyll a fluorescence induction) and photosystem II: basics and applications of the OJIP fluorescence transient. *Journal of Photochemistry and Photobiology B: Biology* **104**: 236–257.

Stirbet A, Govindjee. **2012.** Chlorophyll a fluorescence induction: a personal perspective of the thermal phase, the J–I–P rise. *Photosynthesis Research* **113**: 15–61.

Stirbet A, Govindjee. **2016.** The slow phase of chlorophyll a fluorescence induction in silico: origin of the S-M fluorescence rise. *Photosynthesis Research* **130**: 193–213.

Stirbet A, Strasser RJ. 1995. Numerical simulation of the fluorescence induction in plants. *Archives des Sciences – Université de Genève* **48**: 41–60.

Stirbet A, Strasser RJ. 1996. Numerical simulation of the in vivo fluorescence in plants. *Mathematics and Computers in Simulation* **42**: 245–253.

Stirbet A, Govindjee, Strasser BJ, Strasser RJ. 1998. Chlorophyll a fluorescence induction in higher plants: modeling and numerical simulation. *Journal of Theoretical Biology* **193**: 131–151.

Stirbet A, Rosenau P, Strőder AC, Strasser RJ. 2001. Parameter optimisation of fast chlorophyll fluorescence induction model. *Mathematics and Computers in Simulation* **56**: 443–450.

Stirbet A, Riznichenko GY, Rubin AB, Govindjee. **2014.** Modeling chlorophyll a fluorescence transient: relation to photosynthesis. *Biochemistry (Mosc.)* **79**: 291–323.

Stirbet A, Lazár D, Kromdijk J, Govindjee. **2018.** Chlorophyll a fluorescence induction: can just a one-second measurement be used to quantify abiotic stress responses? *Photosynthetica* **56**: 86–104.

Stirbet A, Lazár D, Papageorgiou CG, Govindjee. **2019.** Chlorophyll a fluorescence in cyanobacteria: relation to photosynthesis. In: Mishra AK, Tiwari DN, Rai AN. eds. *Cyanobacteria – from basic science to applications*. London: Academic Press, 79–130.

Strand DD, Kramer DM. 2014. Control of non-photochemical exciton quenching by the proton circuit of photosynthesis. In: Demmig-Adams B, Garab G, Adams WW III, Govindjee, Sharkey TD, eds. *Nonphotochemical quenching and energy dissipation in plants, algae and cyanobacteria. Advances in photosynthesis and respiration*, vol. 40. Dordrecht: Springer, 387–408.

Strand DD, Fisher N, Davis GA, Kramer DM. 2016. Redox regulation of the antimycin A sensitive pathway of cyclic electron flow around photosystem I in higher plant thylakoids. *Biochimica et Biophysica Acta* **1857**: 1–6

Strand DD, Fisher N, Kramer DM. 2017. The higher plant plastid NAD(P) H dehydrogenase-like complex (NDH) is a high efficiency proton pump that increases ATP production by cyclic electron flow. *The Journal of Biological Chemistry* **292**: 11850–11860.

Strasser RJ. 1978. The grouping model of plant photosynthesis. In: Argyroudi-Akoyunoglou JH, Akoyunoglou G, eds. *Chloroplast development*. Amsterdam: Elsevier Biomedical, 513–515.

Strasser RJ, Govindjee. 1991. The F_0 and the O-J-I-P fluorescence rise in higher plants and algae. In: Argyroudi-Akoyunoglou JH, ed. *Regulation of chloroplast biogenesis*. New York: Plenum Press, 423–426.

Strasser RJ, Stirbet A, 1998. Heterogeneity of photosystem II probed by the numerically simulated chlorophyll *a* fluorescence rise (O-J-I-P). *Mathematics and Computers in Simulation* **48**: 3–9.

Strasser RJ, Stirbet A. 2001. Estimation of the energetic connectivity of PS II centres in plants using the fluorescence rise O-J-I-P. Fitting of experimental data to three different PS II models. *Mathematics and Computers in Simulation* **56**: 451–461.

Strasser RJ, Srivastava A, Govindjee. 1995. Polyphasic chlorophyll a fluorescence transient in plants and cyanobacteria. *Photochemistry and Photobiology* **61**: 32–42.

Strasser RJ, Tsimilli-Michael M, Srivastava A. 2004. Analysis of the chlorophyll fluorescence transient. In: Papageorgiou GC, Govindjee. eds. *Chlorophyll a fluorescence: a signature of photosynthesis. Advances in photosynthesis and respiration*, vol. 19. Dordrecht: Springer, 321–362.

Sušila P, Lazár D, Ilík P, Tomek P and Nauš J. 2004. The gradient of exciting radiation within a sample affects relative heights of steps in the fast chlorophyll *a* fluorescence rise. *Photosynthetica* **42**: 161–172.

Sylak-Glassman EJ, Zaks J, Amarnath K, Leuenberger M, Fleming GR. 2016. Characterizing non-photochemical quenching in leaves through fluorescence lifetime snapshots. *Photosynthesis Research* **127**: 69–76.

Tagawa K, Tsujimoto HY, Arnon DI. 1963. Role of chloroplast ferredoxin in the energy conversion process of photosynthesis. *Proceedings of the National Academy of Sciences of the USA* **49**: 567–572.

Thompson LK, Brudvig GW. 1988. Cytochrome b-559 may function to protect photosystem II from photoinhibitin. *Biochemistry* **27**: 6653–6658.

Tian L, Xu P, Chukhutsina VU, Holzwarth AR, Croce R. 2017. Zeaxanthin-dependent nonphotochemical quenching does not occur in photosystem I in the higher plant *Arabidopsis thaliana*. *Proceedings of the National Academy of Sciences of the USA* **114**: 4828–4832.

Tikhonov AN. 2013. pH-Dependent regulation of electron transport and ATP synthesis in chloroplasts. *Photosynthesis Research* **116**: 511–534.

Tikhonov AN, Vershubskii AV. 2014. Computer modeling of electron and proton transport in chloroplasts. *Biosystems* **121**: 1–21.

Tokarčík A. 2012. *Rewriting complex biological models in stochastic process algebras. A case study*. Bachelor Thesis, Masaryk University.

Tomek P, Lazár D, Ilík P, Nauš J. 2001. On the intermediate steps between the O and P steps in chlorophyll *a* fluorescence rise measured at different intensities of exciting light. *Australian Journal of Plant Physiology* **28**: 1151–1160.

Tomek P, Ilík P, Lazár D, Štroch M, Nauš J. 2003. On the determination of Q_B-non-reducing photosystem II centers from chlorophyll *a* fluorescence induction. *Plant Science* **164**: 665–670.

Trebst A, Reimer S. 1973. Energy conservation in photoreductions by Photosystem II. Reversal of dibromothymoquinone inhibition of Hill-reactions by phenylenediamines. *Zeitschrift für Naturforschung* **28c**: 710.

Trissl H-W, Lavergne J. 1995. Fluorescence induction from photosystem II: analytical equations for the yields of photochemistry and fluorescence derived from analysis of a model including exciton-radical pair equilibrium and restricted energy transfer between units. *Australian Journal of Plant Physiology* **22**: 183–193.

Trissl H-W, Gao Y, Wulf K. 1993. Theoretical fluorescence induction curves derived from coupled differential equations describing the primary photochemistry of photosystem II by an exciton-radical pair equilibrium. *Biophysical Journal* **64**: 974–988.

Tyystjärvi E. 2013. Photoinhibition of photosystem II. *International Review of Cell and Molecular Biology* **300**: 243–303.

Tyystjärvi E, Hakala M, Sarvikas P. 2005. Mathematical modelling of the light response curve of photoinhibition of photosystem II. *Photosynthesis Research* **84**: 21–27.

Valero E, Gonzalez-Sanchez MI, Macia H, Garcıa-Carmona F. 2009. Computer simulation of the dynamic behavior of the glutathione-ascorbate redox cycle in chloroplasts. *Plant Physiology* **149**: 1958–1969.

van Amerongen H, Croce R. 2013. Light-harvesting in photosystem II. *Photosynthesis Research* **116**: 251–263.

van Gorkom HJ. 1974. Identification of the reduced primary electron acceptor of Photosystem II as a bound semiquinone anion. *Biochimica et Biophysica Acta* **347**: 439–442.

van Gorkom HJ, Pulles MPJ, Etienne A-L. 1978. Fluorescence and absorbance changes in Tris-washed chloroplasts. In: Metzner H, ed. *Photosynthetic oxygen evolution*. London: Academic Press, 135–145.

van Kooten O, Snel JFH, Vredenberg VJ. 1986. Photosynthetic free energy transduction related to the electric potential changes across the thylakoid membrane. *Photosynthesis Research* **9**: 211–227.

van Rensen JJS. 2002. Role of bicarbonate at the acceptor side of Photosystem II. *Photosynthesis Research* **73**: 185–192.

Vavilin DV, Tyystjärvi E, Aro E-M. 1998. Model for the fluorescence induction curve of photoinhibited thylakoids. *Biophysical Journal* **75**: 503–512.

Velthuys BR, Amesz J. 1974. Charge accumulation at the reducing side of Photosystem 2 of photosynthesis. *Biochimica et Biophysica Acta* **333**: 85–94.

Vermaas WFJ. 2007. Targeted genetic modification of cyanobacteria: new biotechnological applications. In: Richmond A, ed. *Handbook of microalgal culture*. Oxford: Blackwell Science, 457–470.

Vermeglio A. 2002. The two-electron gate in photosynthetic bacteria. *Photosynthesis Research* **73**: 83–86.

Vink M, Zer H, Alumot N, *et al.* 2004. Light modulated exposure of the light-harvesting complex II (LHCII) to protein kinase(s) and state transition in *Chlamydomonas reinhardtii* xanthophyll mutants. *Biochemistry* **43**: 7824–7833.

Visser D, Heijnen J. 2002. The mathematics of metabolic control analysis revisited. *Metabolic Engineering* **4**: 114–123.

Vredenberg WJ. 2000. A three-state model for energy trapping and chlorophyll fluorescence in photosystem II incorporating radical pair recombination. *Biophysical Journal* **79**: 26–38.

Vredenberg WJ. 2008. Algorithm for analysis of OJDIP fluorescence induction curves in terms of photo- and electrochemical events in photosystems of plant cells. Derivation and application. *Journal of Photochemistry and Photobiology B: Biology* **91**: 58–65.

Vredenberg WJ. 2011. Kinetic analyses and mathematical modeling of primary photochemical and photoelectrochemical processes in plant photosystems. *BioSystems* **103**: 138–151.

Vredenberg WJ, Duysens LNM. 1963. Transfer of energy from bacteriochlorophyll to a reaction centre during bacterial photosynthesis. *Nature* **197**: 355–357.

Wang X, Cao J, Maroti P, *et al.* 1992. Is bicarbonate in photosystem II the equivalent of the glutamate ligand to the iron atom in bacterial reaction centers? *Biochimica et Biophysica Acta* **1100**: 1–8.

Warburg O, Uyesugi T. 1924. Über die Blackmansche Reaktion. *Biochemische Zeitschrift* **146**: 486–492.

Werdan K, Heldt HW, Milovancev M. 1975. The role of pH in the regulation of carbon fixation in the chloroplast stroma. Studies on CO_2 fixation in the light and dark. *Biochimica et Biophysica Acta* **396**: 276–292.

Wientjes E, Croce R. 2012. PMS: photosystem I electron donor or fluorescence quencher. *Photosynthesis Research* **111**: 185–191.

Willstätter R, Stoll A. 1913. *Untersuchungen über Chlorophyll*. Berlin: Justus Springer.

Witt HT. 2004. Steps on the way to building blocks, topologies, crystals and X-ray structural analysis of Photosystems I and II of water-oxidizing photosynthesis. *Photosynthesis Research* **80**: 85–107.

Witt HT, Müller A, Rumberg B. 1961*a*. Experimental evidence for the mechanism of photosynthesis. *Nature* **191**: 194–195.

Witt HT, Müller A, Rumberg B. 1961*b*. Oxidized cytochrome and chlorophyll in photosynthesis. *Nature* **192**: 967–969.

Wood WH, Barnett SFH, Flannery S, Hunter CN, Johnson MP. 2019. Dynamic thylakoid stacking is regulated by LHCII phosphorylation but not its interaction with photosystem I. *Plant Physiology* **180**: 2152–2166.

Wraight CA, Crofts AR. 1970. Energy-dependent quenching of chlorophyll a fluorescence in isolated chloroplasts. *European Journal of Biochemistry* **17**: 319–327.

Wydrzynski T, Govindjee. 1975. A new site of bicarbonate effect in Photosystem II of photosynthesis; evidence from chlorophyll fluorescence transients in spinach chloroplasts. *Biochimica et Biophysica Acta* **387**: 403–408.

Wydrzynski T, Satoh K, eds. 2005. *Photosystem II: the light-driven water-plastoquinone oxidoreductase. Advances in photosynthesis and respiration*, Vol. 22. Dordrecht: Springer.

Xia Q, Tan J, Ji X, Jiang Y, Guo Y. 2018. Modelling and simulation of chlorophyll fluorescence from photosystem II as affected by temperature. *IET Systems Biology* **12**: 304–310.

Xin CP, Yang J, Zhu XG. 2013. A model of chlorophyll *a* fluorescence induction kinetics with explicit description of structural constraints of individual photosystem II units. *Photosynthesis Research* **117**: 339–354.

Yamamoto HY, Higashi RM. 1978. Violaxanthin deepoxidase. Lipid composition and substrate specificity. *Archives of Biochemistry and Biophysics* **190**: 514–522.

Yamamoto HY, Nakayama T, Chichester C. 1962. Studies on the light and dark interconversions of leaf xanthophylls. *Archives of Biochemistry and Biophysics* **97**: 168–173.

Yamori W, Makino A, Toshiharu Shikanai T. 2016. A physiological role of cyclic electron transport around photosystem I in sustaining photosynthesis under fluctuating light in rice. *Scientific Reports* **6**: 20147.

Yin X, Harbinson J, Struik PC. 2009. A model of the generalized stoichiometry of electron transport limited C3 photosynthesis: development and applications. In: Laisk A, Nedbal AL, Govindjee, eds. *Photosynthesis in silico: understanding complexity from molecules to ecosystems. Advances in photosynthesis and respiration*, Vol. 29. Dordrecht: Springer, 247–273.

Zaks J, Amarnath K, Kramer DM, Niyogi KK, Fleming GR. 2012. A kinetic model of rapidly reversible nonphotochemical quenching. *Proceedings of the National Academy of Sciences of the USA* **109**: 15757–15762.

Zaks J, Amarnath K, Sylak-Glassman EJ, Fleming GR. 2013. Models and measurements of energy-dependent quenching. *Photosynthesis Research* **116**: 389–409.

Zhou Y, Schideman LC, Park DS, *et al.* 2015. Characterization of a *Chlamydomonas reinhardtii* mutant strain with improved biomass production under low light and mixotrophic conditions. *Algal Research* **11**: 134–147.

Zhu XG, Govindjee, Baker NR, deSturler E, Ort DR, Long SP. 2005. Chlorophyll *a* fluorescence induction kinetics in leaves predicted from a model describing each discrete step of excitation energy and electron transfer associated with photosystem II. *Planta* **223**: 114–133.

Zhu XG, de Sturler E, Long SP. 2007. Optimizing the distribution of resources between enzymes of carbon metabolism can dramatically increase photosynthetic rate: a numerical simulation using an evolutionary algorithm. *Plant Physiology* **145**: 513–526.

Zhu XG, Long SP, Ort DR. 2010. Improving photosynthetic efficiency for greater yield. *Annual Review of Plant Biology* **61**: 235–261.

Zhu XG, Wang Y, Ort DR, Long SP. 2013. e-Photosynthesis: a comprehensive dynamic mechanistic model of C3 photosynthesis: from light capture to sucrose synthesis. *Plant, Cell & Environment* **36**: 1711–1727.

Zhu XG, Lynch JP, LeBauer DS, Millar AJ, Stitt M, Long SP. 2016. Plants in silico: why, why now and what? – an integrative platform for plant systems biology research. *Plant, Cell & Environment* **39**: 1049–1057.

Zito F, Finazzi G, Delosme R, Nitschke W, Picot D, Wollman FA. 1999. The Qo site of cytochrome b6f complexes controls the activation of the LHCII kinase. *EMBO Journal* **18**: 2961–2969.

Zouni A, Witt HT, Kern J, *et al.* 2001. Crystal structure of photosystem II from *Synechococcus elongatus* at 3.8 Å resolution. *Nature* **409**, 739–743.